

WCAP-14808
REVISION 5

**NOTRUMP Final Validation
Report for AP600**

August 1998

R. L. Fittante
A. F. Gagnon
K. E. Halac
L. E. Hochreiter
J. Iyengar
R. M. Kemper
D. A. Kester
K. F. McNamee
P. E. Meyer
R. A. Osterrieder
R. F. Wright
M. Y. Young

9809210165 980813
PDR ADOCK 05200003
A PDR

Westinghouse Electric Company
Energy Systems
P.O. Box 355
Pittsburgh, PA 15230-0355

© 1998 Westinghouse Electric Company
All Rights Reserved

WESTINGHOUSE NON-PROPRIETARY CLASS 3

WCAP-14808
REVISION 5

**NOTRUMP Final Validation
Report for AP600
Volume 2**

August 1998

R. L. Fittante
A. F. Gagnon
K. E. Halac
L. E. Hochreiter
J. Iyengar
R. M. Kemper
D. A. Kester
K. F. McNamee
P. E. Meyer
R. A. Osterrieder
R. F. Wright
M. Y. Young

Westinghouse Electric Company
Energy Systems
P.O. Box 355
Pittsburgh, PA 15230-0355

© 1998 Westinghouse Electric Company
All Rights Reserved

WESTINGHOUSE NON-PROPRIETARY CLASS 3

WCAP-14808

REVISION 5

**NOTRUMP Final Validation
Report for AP600
Volume 3**

August 1998

R. L. Fittante
A. F. Gagnon
K. E. Halac
L. E. Hochreiter
J. Iyengar
R. M. Kemper
D. A. Kester
K. F. McNamee
P. E. Meyer
R. A. Osterrieder
R. F. Wright
M. Y. Young

Westinghouse Electric Company
Energy Systems
P.O. Box 355
Pittsburgh, PA 15230-0355

© 1998 Westinghouse Electric Company
All Rights Reserved

1.7 Two-Phase Flow Model

To calculate the vapor and liquid flow rates, NOTRUMP solves a mixture momentum equation and uses constitutive relationships (referred to here as a "drift flux model") to separate the mixture into its vapor and liquid components.

1.7.1 Model Description

a) Mixture momentum equation

The one-dimensional mixture momentum equation for a vertical pipe can be written (Reference 1-3):

$$\frac{\partial G_M}{\partial t} + \frac{1}{A} \frac{\partial A \rho_M U_M^2}{\partial x} + \frac{1}{A} \frac{\partial A \rho_l U_r^2}{\partial x} = - \frac{dP}{dx} - \frac{P_w \tau_w}{A} - \rho_M g \quad (1.7-1)$$

where the subscript M denotes mixture, w denotes wall, U_r denotes relative velocity (ft./sec), and:

$$\rho_r = \frac{\alpha(1-\alpha)\rho_v\rho_l}{\rho_M} \quad (1.7-2a)$$

$$G_M = \rho_M U_M \quad (1.7-2b)$$

where the subscript v denotes the vapor region and l denotes the liquid region.

The second and third terms on the left-hand side are the momentum flux terms due to area change and mixture velocity and density gradients, including the effects of relative velocity between the phases. In the NOTRUMP application to AP600, these momentum flux terms are ignored. This assumption is evaluated in Section 1.7.5.

The wall friction term in two-phase flow (second term on the right-hand side) for flow qualities up to 90 percent is evaluated in NOTRUMP by assuming that the flow is all liquid, then applying a two-phase friction multiplier:

$$\left(\frac{dP}{dz} \right)_F = \frac{P_w \tau_w}{A} \approx \frac{1}{2} \left(\frac{f}{D} \right)_{lo} \frac{G_M^2}{\rho_l} \Phi_{lo}^2 \quad (1.7-3)$$

where f is the friction factor and D is the pipe diameter (ft.). The correlation used for two-phase hydraulic loss is discussed in Section 1.9. For flow qualities above 90 percent, a linear transition is assumed to all vapor flow (Section 2.16).

With the above simplifications and after integrating over a flowlink length Δx , the NOTRUMP momentum equation becomes:

$$\frac{\partial G_M}{\partial t} = -\Delta P - \frac{1}{2} \left(f \frac{\Delta x}{D} \right) \frac{G_M^2}{\rho_l} \Phi_{io}^2 - \rho_M g \Delta x \quad (1.7-4)$$

A more convenient form of the momentum equation for numerical solution is in terms of volumetric flow. Consider the phasic mass conservation equations:

$$\frac{\partial \alpha \rho_v}{\partial t} + \frac{1}{A} \frac{\partial A \alpha \rho_v U_v}{\partial x} = \Gamma''' \quad (1.7-5a)$$

$$\frac{\partial (1 - \alpha) \rho_l}{\partial t} + \frac{1}{A} \frac{\partial A (1 - \alpha) \rho_l U_l}{\partial x} = -\Gamma''' \quad (1.7-5b)$$

Where Γ''' is the vapor generation rate per unit volume (lb/ft.³/sec.).

Expand the phase conservation equations as follows:

$$\rho_v \frac{\partial \alpha}{\partial t} + \alpha \frac{\partial \rho_v}{\partial t} + \frac{\rho_v}{A} \frac{\partial A \alpha U_v}{\partial x} + \alpha U_v \frac{\partial \rho_v}{\partial x} = \Gamma''' \quad (1.7-6a)$$

$$\rho_l \frac{\partial (1 - \alpha)}{\partial t} + (1 - \alpha) \frac{\partial \rho_l}{\partial t} + \frac{\rho_l}{A} \frac{\partial A (1 - \alpha) U_l}{\partial x} + (1 - \alpha) U_l \frac{\partial \rho_l}{\partial x} = -\Gamma''' \quad (1.7-6b)$$

Then, dividing by vapor and liquid density respectively, noting that the $d\alpha/dt$'s cancel, assuming that the rate of change of phase densities is small, and adding results in the volumetric flow equation:

$$\frac{1}{A} \frac{\partial A j}{\partial x} = \Gamma''' \left(\frac{1}{\rho_v} - \frac{1}{\rho_l} \right) \quad (1.7-7)$$

The types of transients to which NOTRUMP is applied involve relatively slow depressurization transients, with insignificant vapor superheating, so that the assumption of nearly uniform phase density is reasonable. It can be seen from Equation 1.7-7 that, if the vapor generation rate is also small, the volumetric flow is insensitive to vapor fraction gradients, unlike the mass flow rate. This means that the volumetric flux at a node boundary remains constant, even though the density at the boundary may undergo a discontinuous change. It is therefore advantageous to solve the momentum equation in terms of volumetric flow (see Section 2.4 for coding details). The approach taken and assumptions made are discussed after introduction of the drift flux model in the next section.

b) Drift flux model

Define the volumetric flux of vapor and liquid, j_v and j_l (ft./sec.), and relative velocity U_r in terms of the local velocities U_v and U_l (ft./sec.):

$$j_v = \alpha U_v \quad (1.7-8a)$$

$$j_l = (1 - \alpha)U_l \quad (1.7-8b)$$

$$U_r = U_v - U_l \quad (1.7-8c)$$

The vapor fraction α is the fraction of the local volume taken up by the vapor phase.

Also define the mixture volumetric flux j , as:

$$j = j_v + j_l \quad (1.7-9)$$

Another relative quantity often used is the drift velocity, V_{gj} . This is defined as the velocity of the vapor U_v relative to the volumetric flux j . It can be shown using the above equations that:

$$V_{gj} = U_v - j = (1 - \alpha)U_r \quad (1.7-10)$$

Rearrangement then gives the following basic equations of the drift flux model in terms of the drift velocity:

$$j_v = \alpha j + \alpha V_{gj} \quad (1.7-11a)$$

$$j_l = (1 - \alpha)j - \alpha V_{gj} \quad (1.7-11b)$$

The above equations are definitions that apply locally. To use these equations in real situations, they must be cast in forms that apply over the entire pipe. Variations in local vapor fraction and mixture velocity across the pipe now become important, and complicate the drift flux equations. How this averaging and separating is done depends to some extent on the flow regime being considered. For example, Equations 1.7-11a and 1.7-11b can be averaged as follows (Reference 1-4):

$$\langle j_v \rangle = \langle \alpha j \rangle + \langle \alpha V_{gj} \rangle \quad (1.7-12a)$$

$$\langle j_l \rangle = \langle (1 - \alpha)j \rangle - \langle \alpha V_{gj} \rangle \quad (1.7-12b)$$

Define a distribution parameter C_0 as:

$$C_o = \frac{\langle \alpha j \rangle}{\langle \alpha \rangle \langle j \rangle} \quad (1.7-13)$$

Applying averaging to the second term of Equations 1.7-12a and 1.7-12b results in a weighted average drift velocity:

$$\langle \alpha V_{gj} \rangle = \langle \alpha \rangle \frac{\langle \alpha V_{gj} \rangle}{\langle \alpha \rangle} \quad (1.7-14a)$$

$$= \langle \alpha \rangle \langle \langle V_{gj} \rangle \rangle \quad (1.7-14b)$$

$$= \langle \alpha \rangle \langle (1 - \alpha) U_r \rangle \quad (1.7-14c)$$

Introducing Equations 1.7-13 and 1.7-14c into Equations 1.7-12a and 1.7-12b gives:

$$\langle j_v \rangle = C_o \langle \alpha \rangle \langle j \rangle + \langle \alpha \rangle \langle \langle V_{gj} \rangle \rangle \quad (1.7-15a)$$

$$\langle j_l \rangle = (1 - C_o \langle \alpha \rangle) \langle j \rangle - \langle \alpha \rangle \langle \langle V_{gj} \rangle \rangle \quad (1.7-15b)$$

When the phases are highly separated, such as in annular flow, averaging across the pipe using Equation 1.7-13 leads to $C_o=1.0$. In these situations, it is sometimes more convenient to use an average drift velocity defined by:

$$\langle V_{gj} \rangle = (1 - \langle \alpha \rangle) \langle U_r \rangle \quad (1.7-16)$$

The corresponding drift flux equations are:

$$\langle j_v \rangle = \langle \alpha \rangle \langle j \rangle + \langle \alpha \rangle \langle V_{gj} \rangle \quad (1.7-17a)$$

$$\langle j_l \rangle = (1 - \langle \alpha \rangle) \langle j \rangle - \langle \alpha \rangle \langle V_{gj} \rangle \quad (1.7-17b)$$

The expression for mass velocity in the pipe becomes:

$$G_M = (\rho_l - \Delta \rho \langle \alpha \rangle) \langle j \rangle - \Delta \rho \langle \alpha \rangle \langle V_{gj} \rangle \quad (1.7-18)$$

In the following sections, it is useful to compare the various drift flux expressions on the same basis. From Equations 1.7-15a/b and 1.7-17a/b, $\langle V_{gj} \rangle$ can be related to $\langle \langle V_{gj} \rangle \rangle$ by:

1.7.3 Vertical Flow Models

a) Low vapor fraction concurrent flow

For a variety of low void fraction conditions, it is found that the drift velocity is a simple function of the phasic properties if the effects of variations in fluid conditions across the pipe are accounted for. This is the case for a variety of flow regimes such as bubbly, slug, and churn turbulent flow (Reference 1-4). C_o in Equation 1.7-13 varies from 1.1 to about 1.3, and $\langle\langle V_{gj} \rangle\rangle$ can be expressed by two equations, one of which applies in small diameter pipes in which slug flow can occur, and one in larger diameter pipes where churn turbulent flow is likely:

$$\langle\langle V_{gj,d} \rangle\rangle = 0.35 \left[\frac{g\Delta\rho D}{\rho_l} \right]^{1/2} \quad (1.7-21a)$$

$$\langle\langle V_{gj,c} \rangle\rangle = 1.53 \left[\frac{\sigma g \Delta\rho}{\rho_l^2} \right]^{1/4} \quad (1.7-21b)$$

Several investigators have correlated vapor fraction in pools. For example, Sudo (Reference 1-5) expressed vapor fraction as a function of several property groups and vapor volumetric flux to some power, assuming that the liquid volumetric flux was negligible in comparison to the vapor flux. He found that the assumption of negligible liquid flux is reasonable for values up to about 1 ft./sec. The data range for this correlation is 1 to 100 atmospheres, and 0.2 to 1.5 ft. diameter. An earlier correlation, derived using similar assumptions, is the Yeh correlation (Reference 1-6), which is used in NOTRUMP. The Yeh correlation is based on rod bundle data, while the Sudo correlation is based primarily on pipes of various diameters. These correlations are compared in Figure 1.7-1. It can be seen that the Yeh correlation agrees reasonably well at low to moderate vapor fractions with the more recent Sudo model. The lower vapor fraction at low values of j_v is expected due to the open nature of the tube bundle, allowing for larger bubbles and larger drift velocities. Although the Sudo correlation database does not extend to diameters typical of some of the AP600 components, extrapolation indicates lower vapor fraction for a given vapor flux, consistent with Yeh. The Sudo model indicates a likely change in flow regime for void fractions exceeding about 0.6 (the flat portion of the curve). Above a volumetric flux of about 20 ft./sec., the Yeh correlation may overpredict the vapor fraction.

These void fraction correlations, which are usually in the form $\alpha = Cj_v^a$, can be put in forms convenient for use in the drift flux model, as long as the vapor fraction is relatively low and the liquid flux is small compared to the vapor flux. Using Equation 1.7-17a, the following equation is obtained (Section 2.3 includes additional coding details):

$$\langle V_{gj} \rangle = \langle \langle V_{gj} \rangle \rangle + (C_o - 1) \langle j \rangle \quad (1.7-19)$$

In the following text, the brackets around the fluxes and the vapor fraction are removed. The brackets around the two forms of the drift velocity are retained.

From Equation 1.7-18, the rate of change of mass flow obtained through the momentum equation is recast in terms of the rate of change of volumetric flow (Section 2.4 contains additional coding details):

$$\frac{\partial A \rho_M U_M}{\partial t} = (\rho_l - \Delta \rho \alpha) \frac{\partial A j}{\partial t} \quad (1.7-20)$$

where transient changes in drift velocity, vapor fraction, and phase density are assumed negligible compared to changes in volumetric flow. Note that these conditions should be approximately true because the drift flux model relies on drift velocities derived from steady-state tests.

1.7.2 Constitutive Relationships

In the next subsections, the forms chosen for the drift velocity and C_o are described. Since the drift flux model must be applied to upward and downward flow in vertical pipes, and also to flow in horizontal pipes, applicable correlations must be used.

In terms of geometry, there are two distinct regions in which two-phase flow must be modeled in the AP600. First, there are various pipes of both vertical and horizontal orientation, ranging from less than 1 in. in diameter to over 2 ft. Since these components contain the most significant hydraulic resistances, the highest mixture velocities are through these pipes.

Another group of components includes large diameter vessels in which pools of two-phase mixture reside. These are all at least several feet in diameter. Because the volumetric flow through the system is roughly conserved and is limited by the piping, fluid velocities in these regions are substantially smaller, and phase separation is more extensive.

The objective of the following subsections is to describe the basis for the drift flux models used in NOTRUMP for flow in vertical and horizontal pipes. Several simple models are described that, though not used explicitly in the NOTRUMP application to AP600, serve to clarify certain features and simplify assumptions of the drift flux model.

$$\tau_{w,l} = \frac{f_{w,l} \rho_l U_l^2}{2} \quad (1.7-25a)$$

$$\tau_l = \frac{f_l \rho_v U_r^2}{2} \quad (1.7-25b)$$

Wallis (Reference 1-9) developed an expression for the interfacial friction factor that is widely used in these types of applications, and that visualizes an increasingly thick liquid film as equivalent to an increasingly rough pipe:

$$f_l = 0.005[1 + 75(1 - \alpha)] \quad (1.7-26)$$

A solution of Equation 1.7-24 to obtain the relative velocity was derived by Ishii (Reference 1-8). The complete equations do not have a simple form, but Ishii simplified them to yield the following equation for $\langle V_{gl} \rangle$:

$$\langle V_{gl} \rangle = \frac{1 - \alpha}{\alpha + 4\sqrt{\rho_v/\rho_l}} \left[j + \sqrt{\frac{g\Delta\rho D(1 - \alpha)}{0.015\rho_l}} \right] \quad (1.7-27)$$

C_o can be defined for this flow regime so that Equation 1.7-27 can be put in a form consistent with Equations 1.7-15a/b. C_o and $\langle\langle V_{gl} \rangle\rangle$ for annular flow, using Equation 1.7-19 are:

$$C_{o,a} = 1 + \frac{1 - \alpha}{\alpha + 4\sqrt{\rho_v/\rho_l}} \quad (1.7-28a)$$

$$\langle\langle V_{gl,a} \rangle\rangle = \frac{1 - \alpha}{\alpha + 4\sqrt{\rho_v/\rho_l}} \sqrt{\frac{g\Delta\rho D(1 - \alpha)}{0.015\rho_l}} \quad (1.7-28b)$$

While the annular C_o and $\langle\langle V_{gl} \rangle\rangle$ are obtained differently from the low void fraction form described by Equations 1.7-13 and 1.7-14c, these terms are both describing the same thing: the slip of one phase relative to the other, in addition to the drift of vapor relative to the mixture as a whole.

The EPRI correlation fits functional forms of C_o and $\langle\langle V_{gl} \rangle\rangle$ to a wide range of data in the high vapor fraction range, so this model is the preferred approach and is used in NOTRUMP. However, the annular model above is used to highlight certain common features of high vapor fraction flow and is also used to justify certain simplifying assumptions.

$$\alpha \langle V_{gj} \rangle = j_v - \alpha j \quad (1.7-22a)$$

$$\langle V_{gj} \rangle = (1 - \alpha) j \sqrt{\alpha} \quad (1.7-22b)$$

$$= \frac{(1 - \alpha) \alpha^{1/2}}{C^{1/a}} \quad (1.7-22c)$$

The EPRI model (Reference 1-7) uses the same basic form of the drift flux model expressed by Equation 1.7-13, but makes the variables $\langle V_{gj} \rangle$ and C_0 functions of the phase fluxes, fluid properties, and hydraulic diameter, and then uses these functions to fit a variety of data. Because of its applicability over a wide range of conditions, the EPRI model is used in modified form in NOTRUMP for nearly all the flow paths in AP600 except for large open areas such as the vessel and CMT. The modifications to the EPRI correlation are based on a review of the model and comparison with the simpler models discussed above and are explained further in a subsequent section.

b) High vapor fraction cocurrent flow

At high vapor fractions, the annular flow regime is likely to exist. A model based on an annular film (Reference 1-8) can be used.

Assume an annular film flowing on the inside of a vertical tube. The simplified momentum equations for each phase are:

$$\left(\frac{dP}{dx} + \rho_v g \right) = \frac{\tau_i P_i}{A \alpha} \quad (1.7-23a)$$

$$\left(\frac{dP}{dx} + \rho_l g \right) = \frac{\tau_{w,l} P_{w,l}}{A(1 - \alpha)} - \frac{\tau_i P_i}{A(1 - \alpha)} \quad (1.7-23b)$$

Where P_i is the interfacial area per unit length (ft.²/ft.), $P_{w,l}$ is the wall surface area in contact with the liquid (ft.²/ft.), τ_i is the interfacial shear stress (force per unit interfacial surface, lbf/ft.²) acting on the vapor, and $\tau_{w,l}$ is the wall shear stress acting on the liquid.

Subtracting one equation from the other eliminates the pressure gradient term and results in:

$$\Delta \rho g = - \frac{\tau_{w,l} P_{w,l}}{A(1 - \alpha)} + \frac{\tau_i P_i}{A \alpha (1 - \alpha)} \quad (1.7-24)$$

τ_i can be expressed in a form similar to the wall shear stress, except that the relative velocity between the vapor and the liquid film is used:

c) Countercurrent flow

One of the most important flow regimes the drift flux model must predict is the countercurrent regime. For situations where condensation is not significant, the most widely accepted flooding model, and that which is used by Westinghouse in safety analysis codes such as NOTRUMP, is based on the Wallis flooding model. The original form of the equation, due to Wallis, is written in dimensionless form as:

$$j_v^{m+2} + m(-j_l^*)^{1/2} = C \quad (1.7-29a)$$

$$j_v^* = \frac{j_v}{J} = \frac{j_v}{\sqrt{\frac{\Delta\rho g D}{\rho_v}}} \quad (1.7-29b)$$

$$j_l^* = \frac{\sqrt{\rho_l/\rho_v} j_l}{J} = \frac{j_l}{\sqrt{\frac{\Delta\rho g D}{\rho_l}}} \quad (1.7-29c)$$

$$J = \sqrt{\frac{\Delta\rho g D}{\rho_v}} \quad (1.7-29d)$$

The characteristic velocity J (ft./sec.) is assumed to be a function of the tube diameter D . As the tube diameter increases, the liquid volumetric flux that can flow downward against a given upward flux of vapor increases. This type of behavior is usually called J^* scaling. The constant C is found to range from 0.7 to 1.0, and the constant m from 0.8 to 1 (Reference 1-10).

Tests at larger scales show that the appropriate length scale for large tubes is not the tube diameter but the Taylor instability wave length:

$$\lambda = \sqrt{\frac{\sigma}{\Delta\rho g}} \quad (1.7-30)$$

When the diameter length scale in J above is replaced by the Taylor length scale, the following characteristic velocity results:

$$K = \left[\frac{\sigma \Delta\rho g}{\rho_v^2} \right]^{1/4} \quad (1.7-31)$$

This characteristic velocity is called the Kutateladze number, and the CCFL behavior under these conditions is called K^* scaling. The nondimensional fluxes, obtained by replacing J with K in

Equation 1.7-29d, are described as k^* . In this case, the liquid downward flux for a given vapor flux remains unchanged as tube diameter increases. For steam/water mixtures ranging from 15 to 1000 psia, K^* scaling should apply for tubes larger than about 2 to 3 in. in diameter.

The constant C changes with tube geometry at large scale. However, wide variations in geometry do not strongly affect the value of C . For flooding through holes in a plate, for example, tests by Bankoff (Reference 1-11) show that the value of C approaches two for large holes and thick plates typical of those in a PWR.

The constant m has been shown to be primarily a function of end conditions and to vary from 0.65 to 0.8 (Reference 1-11).

In summary, the CCFL data without condensation at small scales (pipe diameter less than 2 in.) can be adequately represented by the following equation and range of constants:

$$j_v^{1/2} + (0.8 \rightarrow 1.0) \left(\frac{\rho_l}{\rho_v} \right)^{1/4} (-j_l)^{1/2} = (0.7 \rightarrow 1.0) J^{1/2} \quad (1.7-32)$$

For large pipes and orifices typical of those in a reactor, the data can be represented by the following equation:

$$j_v^{1/2} + (0.7 \rightarrow 1.0) \left(\frac{\rho_l}{\rho_v} \right)^{1/4} (-j_l)^{1/2} = (1.5 \rightarrow 2.0) K^{1/2} \quad (1.7-33)$$

When plotted on the $(j_v)^{1/2}$ and $(j_l)^{1/2}$ plane, the above equations are straight lines and define the boundary between permitted countercurrent flow and forbidden countercurrent flow. A two-phase flow computer model, be it drift flux or two fluid, should not predict countercurrent flow in the forbidden region.

Several approaches can be taken to derive a CCFL model applicable at all scales (Reference 1-12). The NOTRUMP vertical CCFL model uses the []^{ac} so that a transition takes place between J^* and K^* scaling as the pipe diameter increases. The constants m and C are 0.7, 1.0 (for small diameter), and 1.79 (for large diameter), respectively, based primarily on large pipe flooding data (Reference 1-13). Equations 1.7-32 and 1.7-33 are used to compare the NOTRUMP flooding predictions using simple pipe models of various diameters (Section 3.2).

In the following, the special forms of $\langle\langle V_{g0} \rangle\rangle$ and C_0 are determined, which cause the drift flux model described by Equations 1.7-15a/b to sweep out the Wallis flooding curve as α is varied, as shown in Figure 1.7-2. In this way, application of the drift flux model leads naturally to the correct limiting rates of countercurrent flow.

Starting with Equations 1.7-15a/b, and letting $\alpha' = \alpha C_0$ and $\alpha \langle V_{gj} \rangle = J_c$, eliminate j to yield:

$$(1 - \alpha')j_v - \alpha'j_l = J_c \quad (1.7-34)$$

Use Equation 1.7-33 to describe the flooding curve, and rewrite Equations 1.7-33 and 1.7-34 as:

$$j_v^{1/2} + (-M_j j_l)^{1/2} - K_c^{1/2} = 0 \quad (1.7-35a)$$

$$(1 - \alpha')j_v - \alpha'j_l - J_c = 0 \quad (1.7-35b)$$

where:

$$M_c = (0.7)^2 \sqrt{\frac{\rho_l}{\rho_v}} \quad (1.7-36a)$$

$$K_c = (1.79)^2 K \quad (1.7-36b)$$

It is relatively straightforward to show (Reference 1-14) that for the drift flux lines to be tangent to the CCFL curve as α is varied, J_c must have the form:

$$J_c = \frac{\alpha'(1 - \alpha')K_c}{\alpha' + M_c(1 - \alpha')} \quad (1.7-37)$$

A relationship must still be found between α' and α . It is observed (Reference 1-13) in large-scale flooding tests that the point of zero liquid downflow ($j_l = 0$) is defined by a characteristic vapor velocity and is independent of the vapor fraction (at high vapor fractions). This characteristic velocity, which also defines the constant K_c in Equation 1.7-35a, is found to be:

$$K_c = 3.2 \left(\frac{\sigma g \Delta \rho}{\rho_v^2} \right)^{1/4} \quad (1.7-38)$$

Setting j_l to zero in Equation 1.7-35b, and using Equation 1.7-37:

$$j_v(j_l=0) = \frac{J_c}{1 - \alpha'} = \frac{\alpha' K_c}{\alpha' + M_c(1 - \alpha')} \quad (1.7-39)$$

Since $j_v = \alpha U_v$, and, at zero liquid penetration, $U_v = K_c$:

$$j_v(j_l=0) = \alpha K_c = \frac{\alpha'^{1.2} K_c}{\alpha' + M_c(1 - \alpha')} \quad (1.7-40)$$

Thus:

$$\alpha = \frac{\alpha'}{\alpha' + M_c(1 - \alpha')} \quad (1.7-41)$$

A multiplier can be defined, called $C_{o,f}$. Using Equations 1.7-37 and 1.7-41:

$$\alpha' = C_{o,f} \alpha \quad (1.7-42a)$$

$$C_{o,f} = \frac{M_c}{1 + (M_c - 1)\alpha} \quad (1.7-42b)$$

$$\langle\langle V_{g,f} \rangle\rangle = \frac{C_{o,f} K_c}{\frac{C_{o,f} \alpha}{1 - C_{o,f} \alpha} + M_c} \quad (1.7-42c)$$

Equations 1.7-42b and 1.7-42c describe a drift flux model that sweeps out the CCFL curve as illustrated in Figure 1.7-2 and, at high vapor fraction, predicts a vapor velocity at the liquid holdup point consistent with the Kutateladze number. The C_o defined by Equation 1.7-42b is derived in a manner different from those defined by Equation 1.7-13 or Equation 1.7-28a. Here, it is simply the form needed to obtain the proper asymptotic behavior of the drift flux lines at the liquid hold up point. Figure 1.7-3 compares $C_{o,s}$ (Equation 1.7-28a) and $C_{o,f}$ as functions of vapor fraction. It can be seen that the behavior is similar, even though $C_{o,s}$ applies to cocurrent flow. This similarity is taken advantage of when the overall model is summarized.

d) Application of EPRI drift flux model

The EPRI drift flux model is used in modified form for all vertical pipes in the RCS, as described below.

The drift velocity and distribution parameters derived from the EPRI correlation, []^{ac} are compared to the flooding model values, []^{ac} from Equations 1.7-42b/c, and the [minimums]^{ac} of each are taken. This forces the countercurrent flooding behavior to be bounded by the CCFL curve, as described by Equations 1.7-32 and 1.7-33. Although the EPRI correlation has provision for calculating countercurrent flow, the approach is more complicated, and the CCFL curve is based only on flooding data through orifice plates. Examination of the drift flux lines produced by the EPRI correlation indicates that a larger countercurrent region is permitted by the unmodified EPRI model. The modified model therefore tends to produce more liquid holdup.

1.7.4 Horizontal Flow Models

a) Cocurrent flow

Several methods have been used to correct homogeneous flow theory for slip effects in horizontal two-phase flow, or high mass velocity cocurrent vertical flows. These methods usually involve flow parameters or a slip ratio to relate flow variables such as flow quality or average volumetric flux to the average vapor fraction. The slip ratio is defined as:

$$S = \frac{\langle U_v \rangle}{\langle U_l \rangle} = \frac{(1 - \langle \alpha \rangle) \langle j_v \rangle}{\langle \alpha \rangle \langle j_l \rangle} \quad (1.7-43)$$

Thom (Reference 1-15) found that the slip ratio was basically a function of the vapor and liquid density ratio, over a wide range of conditions. The table below summarizes Thom's data.

Slip Ratio in Two-Phase Mixtures Determined by Thom

Density Ratio (ρ_l / ρ_v)	Slip Ratio
10	1.5
100	2.7
500	4.2
1000	5.5

Others (Reference 1-16) have used the flow parameter K, defined as:

$$\alpha = K \frac{j_v}{j_v + j_l} \quad (1.7-44)$$

Typical values of K are on the order of 0.8.

Both the slip ratio and the flow parameter can be expressed in terms of a horizontal $C_{o,h}$, defined below:

$$j_v = C_{o,h} \alpha j \quad (1.7-45a)$$

$$j_l = (1 - C_{o,h} \alpha) j \quad (1.7-45b)$$

Substituting Equation 1.7-43 into Equation 1.7-45a:

$$S = \frac{(1 - \alpha) C_{o,h} \alpha j}{\alpha (1 - C_{o,h} \alpha) j} \quad (1.7-46)$$

Rearranging, C_o becomes:

$$C_{o,h} = \frac{S}{1 + (S - 1) \alpha} \quad (1.7-47)$$

From Equation 1.7-44, $K = 1/C_{o,B}$.

The values of $C_{o,c}$ and $C_{o,B}$ calculated from Thom's data and from the flow parameter K are plotted in Figure 1.7-4 and are compared with the low vapor fraction vertical flow form $C_{o,c}$ ($C_{o,c} = 1.2$ to 1.3) and the high vapor fraction form, $C_{o,a}$ (Equation 1.7-28a) at atmospheric pressure. It can be seen that the value of $C_{o,B}$ from the Bankoff model ($1/K = 1.25$) is similar to that obtained for low vapor fraction vertical flow, and the $C_{o,h}$ obtained from the Thom data is similar to the annular flow model, $C_{o,a}$ (and from Figure 1.7-3, also to the CCFL model, $C_{o,f}$).

This similarity suggests that both vertical and horizontal concurrent flows can be described with the same model for C_o . For low vapor fraction flows, a constant value of 1.25 would apply; for annular or stratified flows, either $C_{o,a}$ or $C_{o,f}$ would apply. When the pipe is in the vertical orientation, the same C_o models can be used; only the applicable $\langle\langle V_{gr} \rangle\rangle$ term needs to be added. This is what is done in the NOTRUMP code.

b) Stratified/countercurrent flow

An important flow regime in horizontal channels is the stratified flow regime. In this flow regime, steam can flow countercurrent to the liquid, and there is little interaction between the phases. An equally important aspect of these flows is the point at which the stratified flow regime transitions to a slug or bubbly regime. When the transition occurs, the interfacial drag between liquid and vapor increases significantly, and the phases are forced to move concurrently.

The flow regime transition from stratified to slug, or plug flow was investigated for square channels by Wallis and Dobson (Reference 1-17). They proposed the following criterion:

$$j_v^* = 0.5\alpha^{3/2} \quad (1.7-48a)$$

$$= \frac{j_v}{\sqrt{\frac{\Delta\rho g D}{\rho_v}}} \quad (1.7-48b)$$

A more complete model for transitions in horizontal flow in circular channels was developed by Dukler and Taitel (Reference 1-18). An expression similar to that obtained by Wallis was developed for the stratified to intermittent boundary, with the constant replaced by a function of the stratified water level.

As pointed out by Takeuchi (Reference 1-19), the stratified to intermittent boundary defined by the above equations is also equivalent to Wallis's solution to the problem of wave stability in horizontal channel flow (Reference 1-9). This solution defines a region of permissible concurrent or countercurrent stratified flow in the j_v, j_l plane in which waves on the water surface remain stable. This region is illustrated in Figure 1.7-5. Outside this region, waves become unstable and cause the flow regime to change. Wallis's form of the equation for the wave stability problem is:

$$j_v^{4/2} + j_l^{4/2} = 1 \quad (1.7-49)$$

For the Duckler-Taitel flow regime transition, the equation is similar in form, but with different exponents:

$$j_v^{4/3} + j_l^{4/3} = 1 \quad (1.7-50)$$

The characteristic velocity is assumed to be a function of the channel diameter D and is equivalent to J in Equation 1.7-29d. In contrast to vertical flow, this relationship is expected to hold at both small and large scales. This is because interfacial disturbances on a horizontal interface are more stable than on a vertical interface, due to the additional stabilizing effect of gravity in the horizontal case.

For the Wallis-Dobson transition, the form is again similar but with different constants and exponents:

$$j_v^{0.3} + j_l^{0.3} = .707 \quad (1.7-51)$$

Equations 1.7-49 to 1.7-51 can be used to represent the stratified flow regime transition boundary. Since Equations 1.7-50 and 1.7-51 more accurately represent the data trends, these are used as benchmarks against which to compare predictions by the NOTRUMP code in Section 3.3.

It should be noted that the limits described by the above equations are stability limits, and as such should be viewed as upper limits to the stratified flow regime. The extent of countercurrent flow is controlled primarily by the level gradients occurring in the pipe, as described below.

The driving force for horizontal countercurrent flow is assumed to be an initial liquid level difference in the channel, as illustrated in Figure 1.7-11. Positive flow is defined from left to right. The liquid experiences an additional force due to the level difference Δh , which is:

$$-A_l \Delta \rho g \Delta h = -A(1 - \alpha) \Delta \rho g \Delta h \quad (1.7-52)$$

A balance is achieved when the interfacial drag is sufficient to offset this force. Integrating Equations 1.7-23a and 1.7-23b and assuming that wall shear is negligible results in:

$$-(\Delta P + \rho_v g \Delta h) = \frac{\tau_i P_i \Delta x}{\alpha A} \quad (1.7-53a)$$

$$-(\Delta P + \rho_l g \Delta h) = -\frac{\tau_i P_i \Delta x}{(1 - \alpha) A} \quad (1.7-53b)$$

This leads to:

$$\Delta \rho g \Delta h = \frac{\tau_i P_i \Delta x}{\alpha(1 - \alpha) A} \quad (1.7-54)$$

The interfacial perimeter P_i (ft.) is approximately proportional to $4\alpha(1-\alpha)D$, reaching a maximum when the pipe is half full, and going to zero at each extreme. Using Equation 1.7-26 for the interfacial friction factor and rearranging leads to:

$$(1 - \alpha)U_r = \left[\frac{(1 - \alpha)^2 \pi}{.04[1 + 75(1 - \alpha)]} \right]^{1/2} \sqrt{\frac{\Delta \rho g (\Delta h / \Delta x) D}{\rho_v}} \quad (1.7-55)$$

For a wide range of vapor fractions at low pressure, the first term on the right hand side is approximately 0.6.

The simple model developed above indicates that the countercurrent flow drift velocity is likely to be substantially lower than the limit established by stability limits, unless the level gradient is on the order of 1.0.

As the mixture flow increases, wall shear is likely to become important. In this case, a slip component enters via C_o , whose form is similar to those obtained for annular flow. To simulate the overall behavior of horizontal flow, the following forms of V_{gj} and C_o are used:

$$\left[\quad \quad \quad \right]^{a,c} \quad (1.7-56a)$$

$$\left[\quad \quad \quad \right]^{a,c} \quad (1.7-56b)$$

where:

$$M_{c,h} = \sqrt{\frac{\rho_l}{\rho_v}} \quad (1.7-57a)$$

$$K_{c,h} = \sqrt{\frac{\Delta \rho g (\Delta h / \Delta x) D}{\rho_v}} \quad (1.7-57b)$$

As indicated in the previous subsection and demonstrated in Figures 1.7-2 and 1.7-3, the above expression for $\left[\quad \right]^{a,c}$ represents concurrent stratified and annular flows reasonably well, while the V_{gj} drift term accounts for countercurrent stratified flow at low mixture flow rates. These forms also result in drift flux lines that sweep out a parabolic countercurrent flow boundary, consistent with the stability limits (although these boundaries are well below the limits defined by Equations 1.7-49, 1.7-50, and 1.7-51).

1.7.5 Effect of Neglecting Momentum Flux Terms

This section provides detailed justification for not including momentum flux in the NOTRUMP models.

NOTRUMP does not include the second and third terms of Equation 1.7-1. The momentum flux terms arise from the acceleration imposed on the flow by density and area changes along the pipe. This can more easily be seen by simplifying the momentum equation to consider steady, horizontal, homogeneous equilibrium flow (the importance of drift or slip effects will be discussed later). The pressure gradient in this case is given by:

$$\frac{dP}{dz} = -\frac{fv_f}{2D} \left(\frac{W}{A}\right)^2 \phi_{10}^2 - \frac{1}{A} \frac{d}{dz} (W_g u_g + W_l u_l) \quad 1.7-58$$

where P is the pressure, f is the friction factor, D is the pipe diameter, W is the mixture mass flow rate (subscripts f and g define the gas and liquid flows), A is the area, v_f is the fluid specific volume (1/density), ϕ is the two phase multiplier, and u is the mixture velocity. Assuming homogeneous ($u_f = u_g$) conditions (the importance of drift or slip effects will be discussed later), the momentum equation becomes:

$$\frac{dP}{dz} = -\frac{fv_f}{2D} \left(\frac{W}{A}\right)^2 \phi_{10}^2 - \frac{W}{A} \frac{du}{dz} \quad 1.7-59$$

Since $u = Wv/A$, where v is the mixture specific volume, the velocity derivative can be replaced to yield:

$$\frac{dP}{dz} = -\frac{fv_f}{2D} G^2 \phi_{10}^2 - G^2 \frac{dv}{dz} + \frac{G^2 v}{A} \frac{dA}{dz} \quad 1.7-60$$

Where $G = W/A$. The above equation separates the influence of changing specific volume, and changing flow area. In two phase flow, the mixture specific volume is given by:

$$v = v_f + xv_g$$

where x is the steam quality. Since the phasic specific volumes are functions of pressure only, the spatial derivative can be split into:

$$\frac{dv}{dz} = \left(\frac{dv_f}{dP} + x \frac{dv_{fg}}{dP} \right) \frac{dP}{dz} + v_{fg} \frac{dx}{dz} = (xv'_g + (1-x)v'_f) \frac{dP}{dz} + v_{fg} \frac{dx}{dz} \quad 1.7-61$$

where v' means the derivative of specific volume with respect to pressure. Combining the above equations yields the following equation (similar to equation 2.44 of Reference 1-21):

$$\frac{dP}{dz} = \frac{- \left(\frac{fv_f}{2D} \phi_{lo}^2 + v_{fg} \frac{dx}{dz} - \frac{v}{A} \frac{dA}{dz} \right) G^2}{1 + G^2 [xv'_g + (1-x)v'_f]} \quad 1.7-62$$

This equation shows that the momentum flux terms influence the pressure gradient locally (via the area and quality gradients in the numerator), and globally via the denominator.

The area change term is accounted for in the NOTRUMP momentum equation by adding an overall loss factor K to the frictional term which calculates the overall loss in pressure across the area change. Typically, area changes in the AP600 piping network are abrupt, and therefore introduce additional irrecoverable losses which must also be accounted for in the loss factor. Application of the momentum flux term shown above evaluates only the recoverable pressure change, and would not be accurate if applied without the additional or offsetting irrecoverable losses.

The quality gradient term is important where there is boiling due to heat transfer or flashing due to a pressure gradient. If the quality gradient is dominated by boiling from a surface, the energy equation gives:

$$W \frac{d(h_f + xh_{fg})}{dz} = q' \quad 1.7-63$$

where h denotes fluid enthalpy and q' is the local linear heat rate (Btu/ft/s). Expanding the derivative (assuming pressure effects are small), the acceleration effect due to boiling becomes:

$$v_{fg} \frac{dx}{dz} = \frac{v_{fg}}{h_{fg}} \frac{(q'/A)}{G} \quad 1.7-64$$

The momentum flux term may be important during the natural circulation period, where mixture density differences drive the flow. Estimates using typical values indicate this term is comparable to

the friction term at low mass velocities in a boiling channel. In NOTRUMP, this component of the overall pressure drop is accounted for via the two phase multiplier correlation, which is derived from a data base which includes data in heated tubes (Reference 1-22, page 57).

NOTRUMP does not account for the increase in the overall pressure gradient resulting from the denominator in Equation 1.7-62. This term is examined in more detail below.

The increase in fluid quality can also be dominated by the pressure gradient. Across an orifice, for example, the fluid enthalpy can be assumed to be fairly constant, such that $x = (h-h_f)/h_{fg}$ where h is constant. Therefore:

$$v_{fg} \frac{dx}{dz} = v_{fg} \frac{\partial}{\partial P} \left(\frac{h-h_f}{h_{fg}} \right) \frac{dP}{dz} = -\frac{v_{fg}}{h_{fg}} (h'_f + xh'_{fg}) \frac{dP}{dz} \quad 1.7-65$$

The quality gradient term in this case appears in the denominator such that:

$$\frac{dP}{dz} = \frac{-\left(\frac{fv_f}{2D} \phi_{10}^2 - \frac{v}{A} \frac{dA}{dz} \right) G^2}{1 + G^2 [x(v'_g - v_{fg} h'_g / h_{fg}) + (1-x)(v'_f - v_{fg} h'_f / h_{fg})]} \quad 1.7-66$$

where as before the h' terms denote derivatives with respect to pressure. The value of the denominator is controlled by mass velocity. At high mass velocities, the denominator becomes less than one and the pressure gradient is increased. The denominator in fact is a measure of the degree to which the flow is approaching critical conditions.

Effect of unequal phase velocity

Equation 1.7-62 and 1.7-66 assume that the liquid and vapor move at the same velocity. Most flows will develop some difference in phasic velocity. The effect of this relative velocity on the pressure gradient will be examined. Because the denominator is important at high mass velocities, and the slip ratio (u_g/u_f) is a more appropriate measure of the flow condition than the relative velocity (u_g-u_f), the effect of unequal phase velocities will be examined using the slip ratio. The mass velocity can be expressed as (Reference 1-21, Equation 3.17):

$$G = \left(\frac{xv_g}{u_g} + \frac{(1-x)v_f}{u_f} \right)^{-1} \quad 1.7-67$$

Let $S = u_g/u_f$. Then:

$$G = \left(\frac{1}{u_f} \right)^{-1} \left(\frac{xv_g}{S} + (1-x)v_f \right)^{-1} = \frac{u_f}{c_f} \quad 1.7-68$$

$$G = \left(\frac{1}{u_g} \right)^{-1} [xv_g + S(1-x)v_f]^{-1} = \frac{u_g}{c_g}$$

Now evaluate the inertia term in Equation 1.7-58 assuming constant area and flow to simplify the derivation, and use the equations above to get:

$$\frac{1}{A} \frac{d}{dz} (W_g u_g + W_f u_f) = G^2 \frac{d}{dz} [x c_g + (1-x) c_f] \quad 1.7-69$$

The expression in square brackets can be rearranged to give:

$$x c_g + (1-x) c_f = xv_g + (1-x)v_f + x(1-x) \left[\left(\frac{1}{S} - 1 \right) v_g + (S-1)v_f \right] \quad 1.7-70$$

Assuming the quality and slip ratio are independent of pressure, the denominator in Equation 1.7-62 is now:

$$1 + G^2 \left\{ xv'_g + (1-x)v'_f + x(1-x) \left[\left(\frac{1}{S} - 1 \right) v'_g + (S-1)v'_f \right] \right\} \quad 1.7-71$$

The effect of the additional terms in Equation 1.7-71 relative to the denominator in Equation 1.7-62 will be examined below.

Calculated mass velocities in AP600

Figures 1.7-7 to 1.7-13 of Reference 1-20 show the vapor and liquid volumetric flux calculated by NOTRUMP in various components of the AP600. These figures indicate that mass velocities are generally quite low except in the ADS lines. It should be noted that the velocity shown for the ADS4 line is higher than actually calculated in NOTRUMP, because the area used to calculate the velocity from the code output volumetric flow rate was about 20 percent smaller than was actually utilized in the NOTRUMP calculation. Nevertheless, fluid velocities are likely to be on the order of several hundreds of feet per second in these lines. Since the mass velocity is likely to be highest in the ADS lines when the valves are open and critical flow exists at the valves, the importance of the denominator in determining the overall pressure drop will be examined at these locations. For simplicity, the compressibility terms in Equations 1.7-62 and 71 will be evaluated; sample calculations indicate the quality terms in Equations 1.7-66 are smaller because of the relatively large value of h_{fg} .

Table 1.7-2 lists fluid saturation properties at various pressures, from which the derivatives are obtained as shown. Table 1.7-3 evaluates the denominator at several pressures and qualities for ADS1-3, and Table 1.7-4 does the same for ADS4 at the lower pressure. For each quality, the mass velocity in the piping approaching the valve is estimated by multiplying the critical mass velocity for the given pressure and quality (using the HEM model) by the area ratio of the valve to the upstream piping. These calculations indicate the following:

- a) For ADS1-3, the pressure gradient leading up to the ADS valves could be underestimated by as much as 9 percent (the denominator ranges from .91 to .99). However, during the important period of low quality two phase flow, when the mixture level is at the top of the pressurizer, the error is substantially smaller. By itself, this difference is not sufficient to explain the differences between predicted and measured mass flow rates which are observed in some of the OSU tests (see response to RAI 440.721(c)).
- b) For ADS4, where two valves are assumed open, Table 1.7-5 indicates that the pressure gradient could be significantly underpredicted during the initial period just after the valves open, when the pressure is high enough that critical conditions exist. This is because the total valve area is comparable to the upstream piping area.

Figure 1.7-6 shows the effect on the denominator of assuming a slip ratio of 6, for the conditions shown in Table 1.7-4. It can be seen that phase slip increases the value of the denominator, and reduces the effect of acceleration on the pressure gradient. This is consistent with the observation that the Moody critical flow model, which assumes a large slip ratio, predicts a higher critical mass velocity than HEM (i.e., acceleration must be greater to produce large pressure gradients and choked conditions). Therefore, the conditions estimated in Tables 1.7-3 and 4 for homogeneous flow are the most severe to be expected.

NOTRUMP model for ADS piping and critical flow

Figure 1.7-7 illustrates the noding used to model the ADS piping and valves in AP600. The piping from the hot leg or pressurizer to the valve is simulated with a fluid node. A portion of the overall line resistance is allocated to the flow link connected to the pressurizer or hot leg. The local static pressure and enthalpy in the ADS piping node, P_o and h_o , are used in the Henry-Fauske and HEM critical flow models to calculate the critical mass velocity (Section 2.17 Reference 1-20). With this modeling, the frictional pressure drop in the piping leading to the ADS valve is accounted for. The HEM model is applied over the short remaining distance to the valve, where the effect of friction can be ignored. However, the NOTRUMP model contains two deficiencies:

- a) The model does not account for acceleration effects in calculating the pressure distribution up to the ADS valve (previous sections).
- b) The model does not account for the effect of significant upstream kinetic energy on the critical flow calculation.

As indicated in the previous section, lack of momentum flux terms in the momentum equation may result in an underprediction of the pressure drop to the ADS valves. In the next section, the effect of ignoring the kinetic energy terms in the calculation of critical flow is examined.

The HEM critical flow model assumes frictionless adiabatic, steady flow and begins with the following simplified mass, energy and momentum conservation equations:

$$dW = 0$$

$$d \left(h + \frac{u^2}{2} \right) = 0$$

$$dP + \rho u du = 0 \quad 1.7-72$$

$$d \left(\int \frac{dP}{\rho} + \frac{u^2}{2} \right) = 0$$

where h is the fluid enthalpy. Because the flow is assumed frictionless and adiabatic, the flow is isentropic. Therefore, either the momentum equation or the energy equation can be replaced by:

$$ds = 0$$

In the HEM, the energy and entropy equations are used. The differentials are expanded to give:

$$h_t + \frac{u_t^2}{2} = h_0 + \frac{u_0^2}{2} \quad 1.7-73$$

$$s_t = s_0$$

where the subscript t represents the conditions at the throat, and the subscript 0 represents conditions at the location where the acceleration to the throat is assumed to begin. Usually this is taken as a location where the kinetic energy is negligible (u_0 is small). Given the stagnation enthalpy and entropy, the stagnation pressure and the conditions at the throat leading to the maximum mass velocity can be determined. In NOTRUMP, the Henry-Fauske and HEM models consist of a series of tables giving critical mass flux as a function of stagnation enthalpy, and stagnation pressure.

In the modeling of the ADS, the effect of a significant kinetic energy component at the start of the process must be examined. To determine what the appropriate stagnation pressure should be, retain the second form of the momentum equation, and expand the differential to yield:

$$\int_{P_0}^{P_t} \frac{dP}{\rho} + \frac{u_t^2 - u_0^2}{2} = 0 \quad 1.7-74$$

Assume that an average density can be defined such that:

$$\int_{P_0}^{P_t} \frac{dP}{\bar{\rho}} = \frac{P_t - P_0}{\bar{\rho}} \quad 1.7-75$$

Then:

$$P_t + \frac{\bar{\rho}u_t^2}{2} = P_0 + \frac{\bar{\rho}u_0^2}{2} \quad 1.7-76$$

This indicates that the "reservoir" pressure should include the recoverable portion of the fluid dynamic pressure at the point where acceleration is to begin.

The momentum equation can be written:

$$d\left(\int \frac{dP}{\rho} + \frac{u^2}{2}\right) = -\frac{1}{\rho} \frac{dP}{dz} dz \quad (1.7.72a)$$

where the term on the right-hand side represents the pressure loss due to friction. This can be approximated as:

$$d\left(P + \frac{\bar{\rho}u^2}{2}\right) = -\frac{dP}{dz} dz$$

Assuming that a location can be found where the dynamic pressure is negligible (location where $P = P_\infty$), then

$$P_o + \frac{\bar{\rho}u_o^2}{2} = P_\infty - \frac{dP}{dz} L \quad (1.7-72b)$$

The NOTRUMP procedure is to calculate the total pressure just upstream of the valve ($P_o + \frac{\bar{\rho}}{2} u_o^2$) from the hot leg or pressurizer (P_∞ , where dynamic pressure is negligible), then solve for the critical flow using the total pressure as the reservoir pressure.

Because of the energies and pressures involved, a significant velocity must exist at point 0 before significant error is introduced. For example, at 50 psia the enthalpy of steam is 1174 Btu/lb. For a 1 percent increase in the total enthalpy, the fluid velocity must be about 770 ft/s. This would indicate that ignoring the kinetic energy terms, as is done in NOTRUMP, would result in negligible error.

To confirm this, an alternate flow calculation was performed on the ADS4 piping system to compare with the NOTRUMP prediction (as noted previously, the effects of compressibility were determined to be most important for this component). For steam flow in a piping system, the effects of compressibility can be taken into account by the use of net expansion factors Y (Reference 1-23). These factors are functions of the pressure difference through the pipe, and the loss coefficient in the pipe (Figure 1.7-8). The flow rate through the pipe is calculated by the following equation (Equation 1-11, Reference 1-23:

$$W_{AD4} = 0.525Yd^2 \sqrt{\frac{(P_{HL} - P_a) \rho_{vHL}}{K}}$$

1.7-77

where d is the pipe diameter in inches. The calculated flow rate through both valves assuming compressible conditions is compared with the incompressible result ($Y=1$) in Figure 1.7-9. To compare with the NOTRUMP AP600 predictions, vapor flow is plotted against hot leg pressure for the ADS4 pipe in Figure 1.7-10. The NOTRUMP values are seen to remain below the calculated value assuming compressible conditions.

A model of the ADS 4 piping from the hot leg to the valves was developed. This model included integration of the complete momentum and energy equations (assuming steady-state, homogeneous conditions). The NOTRUMP predictions were compared to this model (see response to RAI 440.796F, part (a)). NOTRUMP predicts similar flows through ADS 4 when the hot leg pressure is high enough to result in choked conditions at the valve. At lower pressures, the flow rate predicted by NOTRUMP was about 20 percent higher. This was attributed to underprediction of two-phase pressure drop in some fittings, such as elbows, and lack of acceleration terms, which is still relatively important. In terms of the total vapor released from the time of ADS 4 opening to IRWS⁷ injection, the effect was relatively small (about 5 percent).

Conclusion:

It is concluded that NOTRUMP has compensating errors in regions where the fluid acceleration is significant. These errors become significant only in the ADS 4 piping where both valves are open. The overall effect, however, is to produce a reasonable estimate of the vapor flow through ADS 4 when compared with more detailed models.

Table 1.7-1
FIGURES DEPICTING RESULTS FROM VERTICAL AND HORIZONTAL FLOW MODELS

Figure No.	Title
1.7-1	Yeh Correlation versus Sudo Correlation
1.7-2	CCFL Curve and Tangent Drift Flux Lines
1.7-3	Comparison of Various Forms of C_0 for Vertical Flow Regime
1.7-4	Comparison of C_0 for Horizontal and Vertical Flow
1.7-5	Flow Regime Transitions in Horizontal Flow
1.7-6	Effect of Slip Ratio on Momentum Flux Equation Denominator
1.7-7	NOTRUMP Noding for ADS Valves
1.7-8	Effect of Compressibility on the Calculated Flowrate Through a Piping System
1.7-9	Effect of Compressibility on ADS 4 Flow vs. Pressure
1.7-10	NOTRUMP Predicted Vapor Flow Compared with Reference 1-23 Calculation
1.7-11	Horizontal Stratified Flow with Level Gradient
1.7-12	Flow Regimes in Hot Leg and Cold Leg (High Pressure, Prior to ADS Opening)
1.7-13	Flow Regimes in Hot Leg and Cold Leg (Intermediate Pressure, Just After ADS Opening)
1.7-14	Flow Regimes in Hot Leg and Cold Leg (Low Pressure)
1.7-15	Flow Regimes in Balance Line (High Pressure, Just Prior to ADS Opening)
1.7-16	Flow Regimes in Balance Line and Pressurizer Surge Line (Intermediate Pressure, Just After ADS Opening)
1.7-17	Flow Regimes in Balance Line and ADS-4 (Low Pressure)
1.7-18	Flow Regimes in Steam Generator Tubes (High Pressure, Just Prior to ADS Opening)

Table 1.7-2
WATER SATURATION PROPERTIES AND DERIVATIVES

PRESS	TSAT	VF	VG	VFG	HF	HG	HFG	VF	VG
40	267.25	0.017151	10.496	10.47885	236.15	1169.8	933.65	0	0
45	274.44	0.017214	9.3988	9.381586	243.52	1172	928.48	1.26E-05	-0.21944
50	281.02	0.017274	8.514	8.496726	250.25	1174.1	923.85	1.2E-05	-0.17696
55	287.08	0.017329	7.785	7.767671	256.4	1175.9	919.5	1.1E-05	-0.1458
60	292.71	0.017383	7.1736	7.156217	262.2	1177.6	915.4	1.08E-05	-0.12228
90	320.28	0.017659	4.8953	4.877641	290.7	1185.3	894.6	0	0
95	324.13	0.0177	4.6514	4.6337	294.7	1186.2	891.5	8.2E-05	-0.04878
100	327.82	0.01774	4.431	4.41326	298.5	1187.2	888.7	8E-06	-0.04408
110	334.79	0.01782	4.0484	4.03058	305.8	1188.9	883.1	8E-06	-0.03826
120	341.27	0.01789	3.7275	3.70961	312.6	1190.4	877.8	7E-06	-0.03209
420	449.4	0.01942	1.1057	1.08628	429.6	1204.7	775.1	0	0
460	458.5	0.01959	1.0092	0.98961	439.8	1204.8	765	4.25E-06	-0.00241
500	467.01	0.01975	0.9276	0.90785	449.5	1204.7	755.2	4E-06	-0.00204
540	475.01	0.0199	0.8577	0.8378	458.7	1204.4	745.7	3.75E-06	-0.00175
580	482.57	0.02006	0.7971	0.77704	467.5	1203.9	736.4	4E-06	-0.00152
600	486.2	0.02013	0.76975	0.74962	471.7	1203.7	732	3.5E-06	-0.00137
620	489.74	0.02021	0.74408	0.72387	475.8	1203.4	727.6	4E-06	-0.00128
980	542.14	0.02152	0.4561	0.43458	539.5	1193.7	654.2	0	0
1020	546.99	0.02166	0.4362	0.41454	545.6	1192.2	646.6	3.5E-06	-0.0005
1000	544.58	0.02159	0.44596	0.42437	542.6	1192.9	650.3	3.5E-06	-0.00049
1060	551.7	0.02181	0.4177	0.39589	551.6	1190.7	639.1	3.75E-06	-0.00046
1100	556.28	0.02195	0.4006	0.37865	557.5	1189.1	631.6	3.5E-06	-0.00043

Table 1.7-3
ACCELERATION EFFECTS IN ADS1-3 PIPING
 (Note: See Table 1.7-5 for nomenclature)

PRESS =	50 AVALVE	0.324	APIPE =	0.6827			
VF' =	1.2E-05		VFG =	8.496726	VF =	0.017274	
VG' =	-0.17696		HFG =	923.85	SLIP =	6	
	X	GCRIT	GRPIPE	V	1+G2V'	STERM	1+G2V'S
	0.01	861	409	-0.00176	0.94	0.0015	0.99
	0.1	283	134	-0.01769	0.93	0.0133	0.98
	0.5	145	69	-0.08847	0.91	0.0369	0.95
	0.9	110	52	-0.15926	0.91	0.0133	0.91
	0.99	106	50	-0.17519	0.91	0.0015	0.91
PRESS =	100						
VF' =	8E.06		VFG =	4.41326	VF =	0.01774	
VG' =	-0.04408		HFG =	888.7	SLIP =	6	
	X	CCRIT	GRPIPE	V	1+G2V'	STERM	1+G2V'S
	0.01	1565	743	-0.00043	0.95	0.0004	0.99
	0.1	539	256	-0.0044	0.94	0.0033	0.98
	0.5	282	134	-0.02204	0.91	0.0092	0.95
	0.9	216	103	-0.03967	0.91	0.0033	0.92
	0.99	207	98	-0.04364	0.91	0.0004	0.91
PRESS =	600						
VF' =	3.5E-06		VFG =	0.74962	VF =	0.02013	
VG' =	-0.00137		HFG =	732	SLIP =	6	
	X	GCRIT	GRPIPE	V	1+G2V'	STERM	1+G2V'S
	0.01	6284	2982	-1E-05	0.98	0.0000	1.00
	0.1	2661	1263	-0.00013	0.95	0.0001	0.99
	0.5	1599	759	-0.00068	0.92	0.0003	0.95
	0.9	1254	595	-0.00123	0.91	0.0001	0.91
	0.99	1204	571	-0.00135	0.90	0.0000	0.91
PRESS =	1000						
VF' =	3.5E-06		VFG =	0.42437	VF =	0.02159	

Table 1.7-3 (cont.)
ACCELERATION EFFECTS IN ADS1-3 PIPING
 (Note: See Table 1.7-5 for nomenclature)

VG' =	-0.00049		HFG =	650.3	SLIP =	6
X	GCRIT	GRIPE	V	1+G2V'	STERM	1+G2V'S
0.01	8633	4097	-1.4E-06	0.99	4.2E-06	1.01
0.1	4177	1983	-4.6E-05	0.96	3.82E-05	0.99
0.5	2639	1252	-0.00024	0.92	0.000106	0.95
0.9	2101	997	-0.00044	0.91	3.82E-05	0.91
0.99	2021	959	-0.00048	0.90	4.2E-06	0.91

Table 1.7-4
ACCELERATION EFFECTS IN ADS1-3 PIPING
 (Note: See Table 1.7-5 for nomenclature)

VF =	3.5E-06			VFG =	0.42437	VF =	0.02159
VG' =	-0.00049			HFG =	650.3	SLIP =	6
	X	GCRIT	GRIPE	V	1+G2V'	STERM	1+G2VS
	0.01	8633	4097	-1.4E-06	0.99	4.3E-06	1.01
	0.1	4177	1983	-4.6E-05	0.96	3.82E-05	0.99
	0.5	2639	1252	-0.00024	0.92	0.000106	0.95
	0.9	2101	997	-0.00044	0.91	3.82E-05	0.91
	0.9	2101	997	-0.00044	0.91	3.82E-05	0.91
	0.99	2021	959	-0.00048	0.90	4.3E-06	0.91

Table 1.7-5
ACCELERATION EFFECTS IN ADS4 PIPING

PRESS =	50 AVALVE	0.527	APIPE =	0.559			
VF' =	1.2E-05		VFG =	8.496726	VF =	0.017274	
VG' =	-0.17696		HFG =	923.85	SLIP =	6	
	X	GCRIT	GRIPE	V	1+G ² V'	STERM	1+G ² VS
	0.01	861	812	-0.00176	0.75	0.0015	0.96
	0.1	283	267	-0.01769	0.73	0.0133	0.93
	0.5	145	136	-0.08847	0.64	0.0369	0.79
	0.9	110	104	-0.15926	0.63	0.0133	0.66
	0.99	106	50	-0.17519	0.63	0.0015	0.63

Nomenclature:

- GCRIT = critical mass flux at ADS valve
- GRIPE = mass flux upstream of the valve = GCRIT*AVALVE/APIPE
- V' = $x v_g' + (1-x) v_r'$
- 1+G²V' = denominator in equation 440.721(h) - 5
- STERM = last term in equation 440.721(h) - 13
- 1+G²VS = equation 440.721(h)-14

1.7.6 Conclusion

To determine whether the NOTRUMP drift flux model is being applied within its range of applicability, flow regime maps were generated using the models of Taitel and Dukler (References 1-18 and 1-24). On these maps were placed calculated liquid and vapor volumetric fluxes from selected components from a NOTRUMP calculation of the AP600 2-in. cold leg break. The results are shown in Figures 1.7-11 to 1.7-18. It can be seen that in general, horizontal pipes are always stratified, while vertical pipes traverse several of the flow regimes discussed in this section. The pressurizer surge line is a special case because it is a slanted, curved pipe. Tests in inclined pipes (Reference 1-25) indicate that the stratified flow regime cannot be maintained in slightly inclined pipes, reverting instead to flow regimes more typical of vertical pipes. The surge line flowlink is therefore modeled as a vertical flowlink, and phasic flows are placed on the vertical flow regime map (see Figure 1.7-16). It can be seen that the expected flow regime is annular in the surge line. Because of the special geometry of the surge line, the NOTRUMP drift flux model may have difficulty predicting the correct phasic flows in this component.

It is concluded that the NOTRUMP drift flux model is applicable in both vertical and horizontal pipes. The surge line may present problems to the model due to its unique geometry. There are also indications that the model predicts excessive liquid holdup (i.e., a restrictive CCFL) relative to data in vertical pipes.

Comparison of Yeh to Sudo Void Fraction Correlation; Atmospheric Pressure

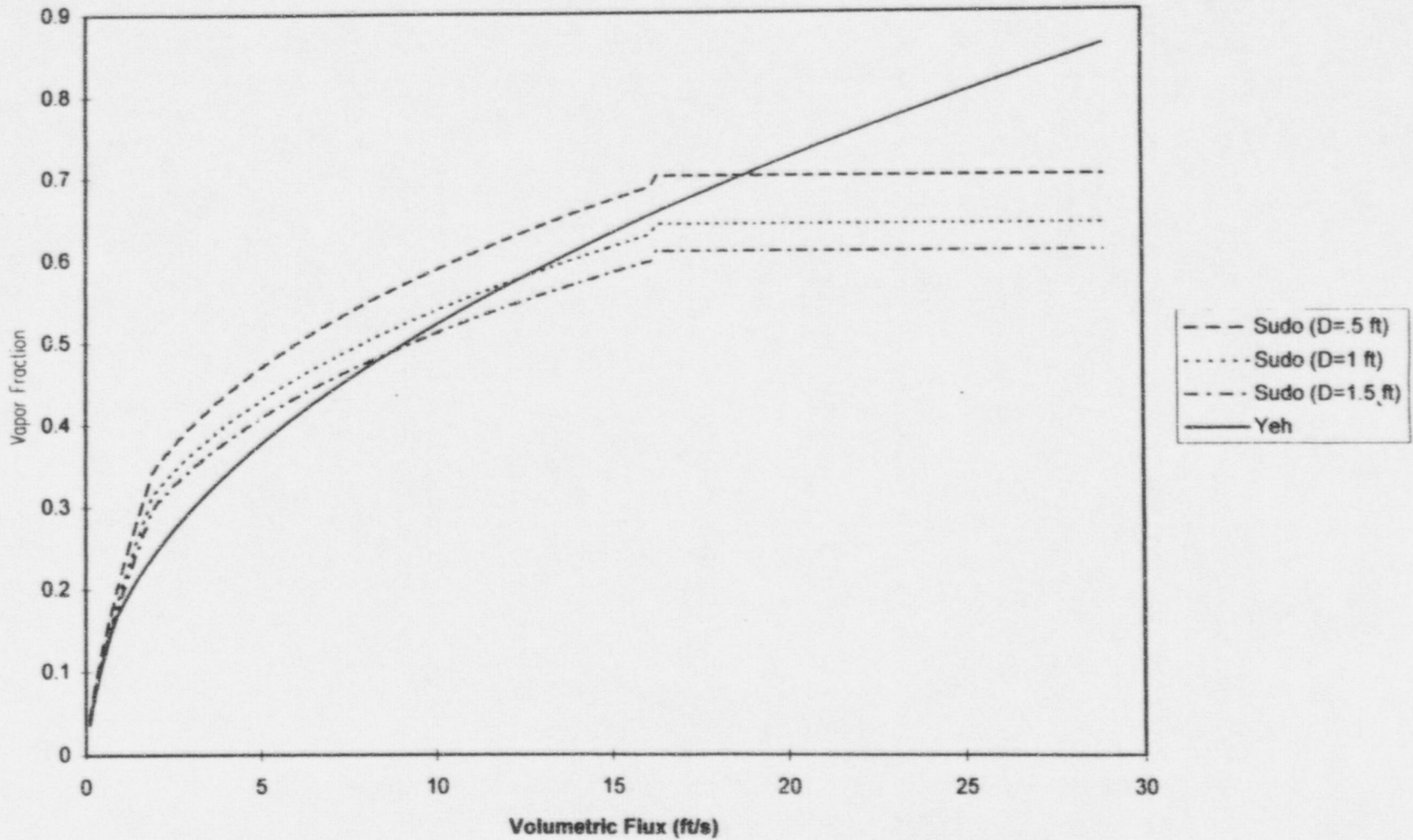


Figure 1.7-1 Yeh Correlation versus Sudo Correlation

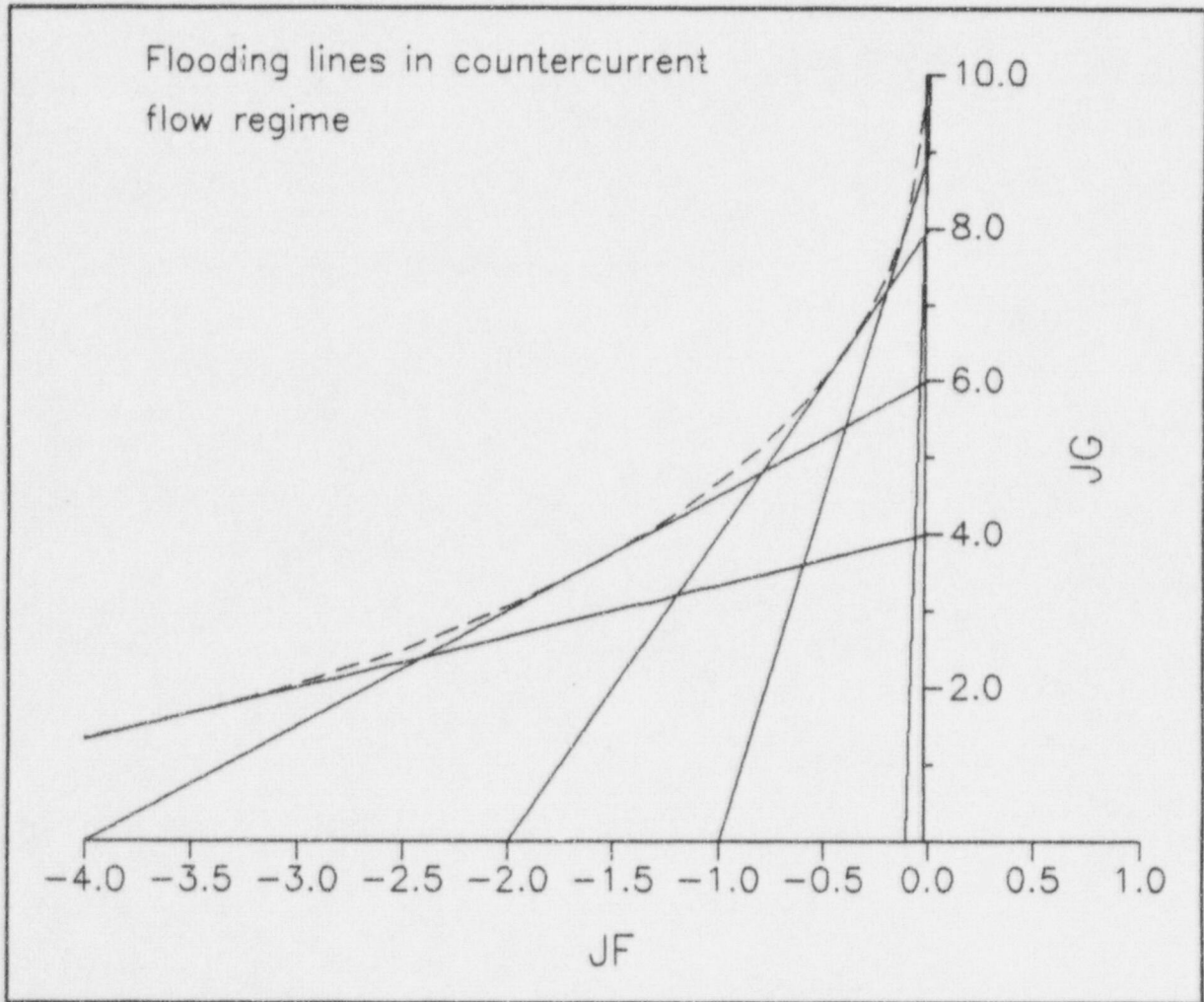


Figure 1.7-2 CCFL Curve and Tangent Drift Flux Lines

COMPARISON OF CO MODELS

ANNULAR CO, α (1) VS FLOODING CO,f (2)

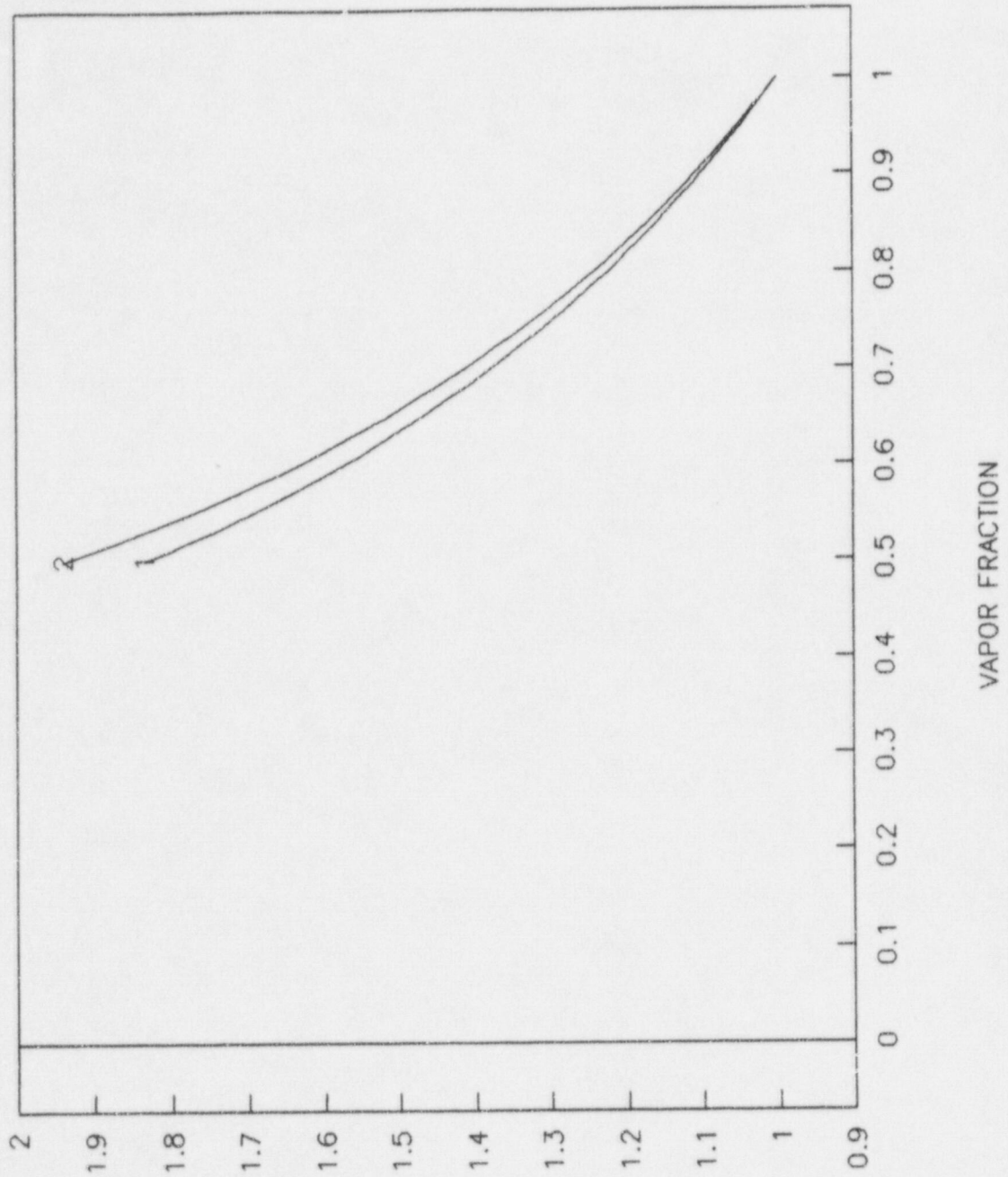


Figure 1.7-3 Comparison of Various Forms of C_o for Vertical Flow Regime

VERTICAL VS HORIZONTAL CO MODELS

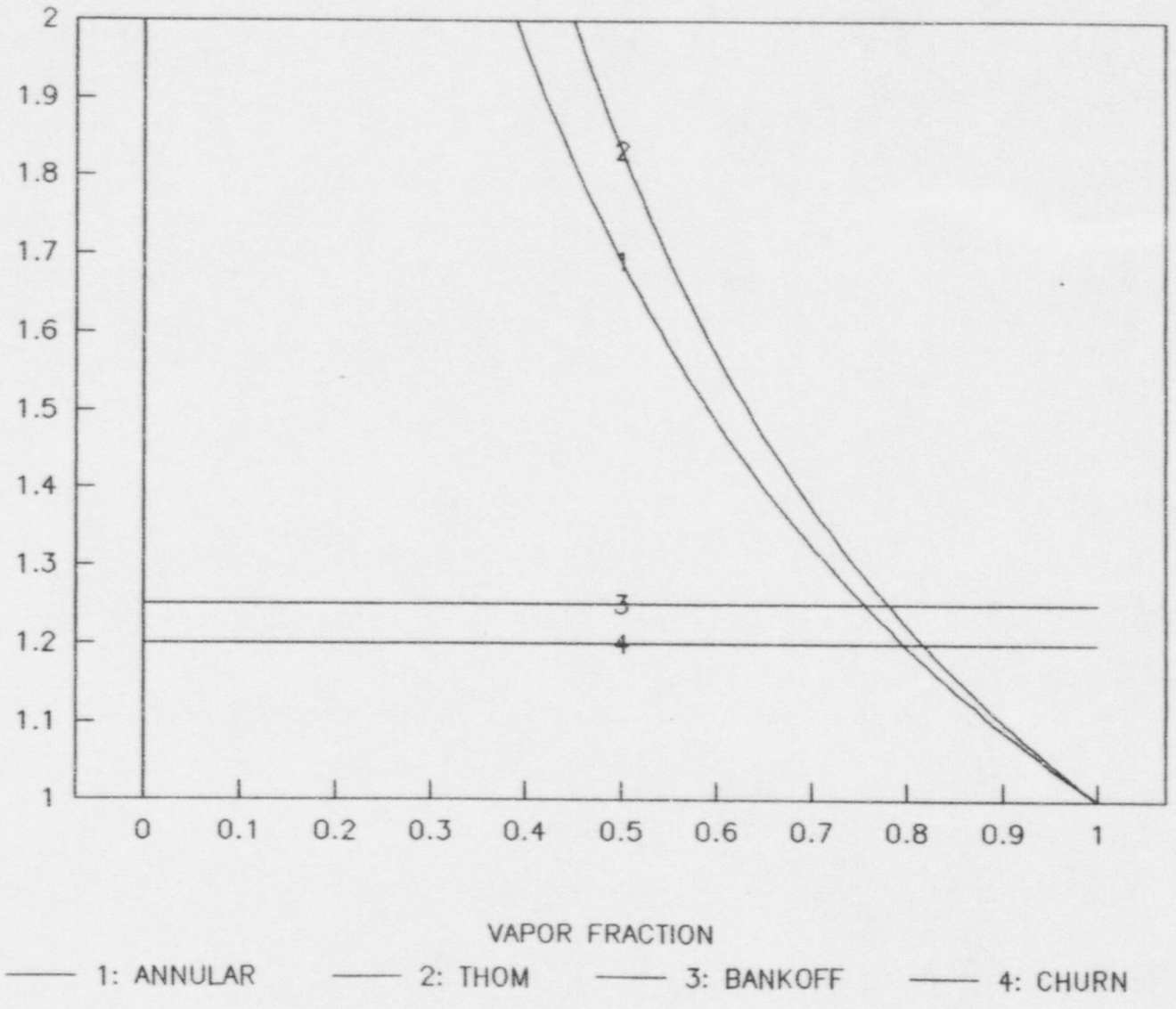


Figure 1.7-4 Comparison of C_o for Horizontal and Vertical Flow

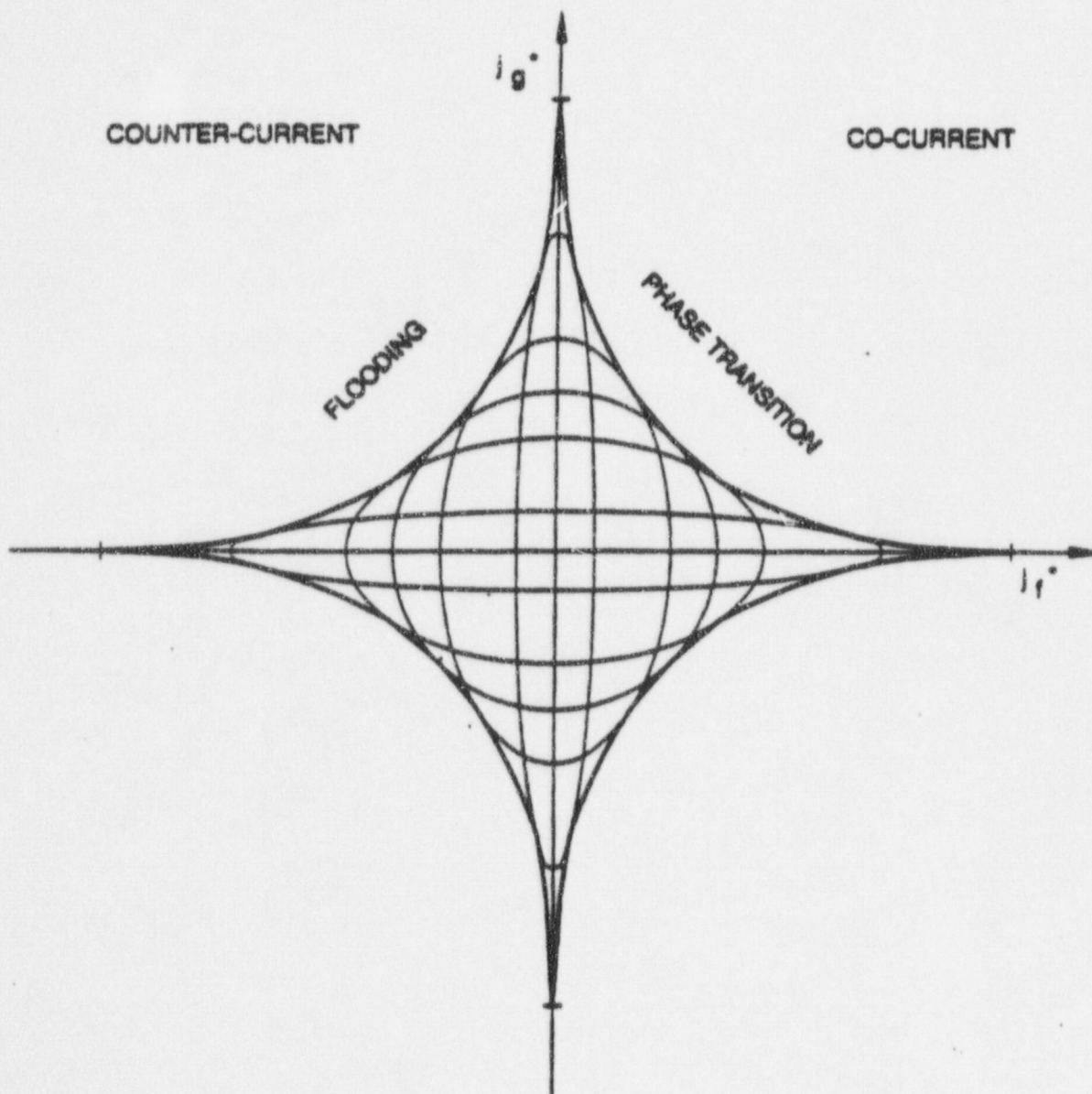


Figure 1.7-5 Flow Regime Transitions in Horizontal Flow

EFFECT OF SLIP RATIO ON DENOMINATOR

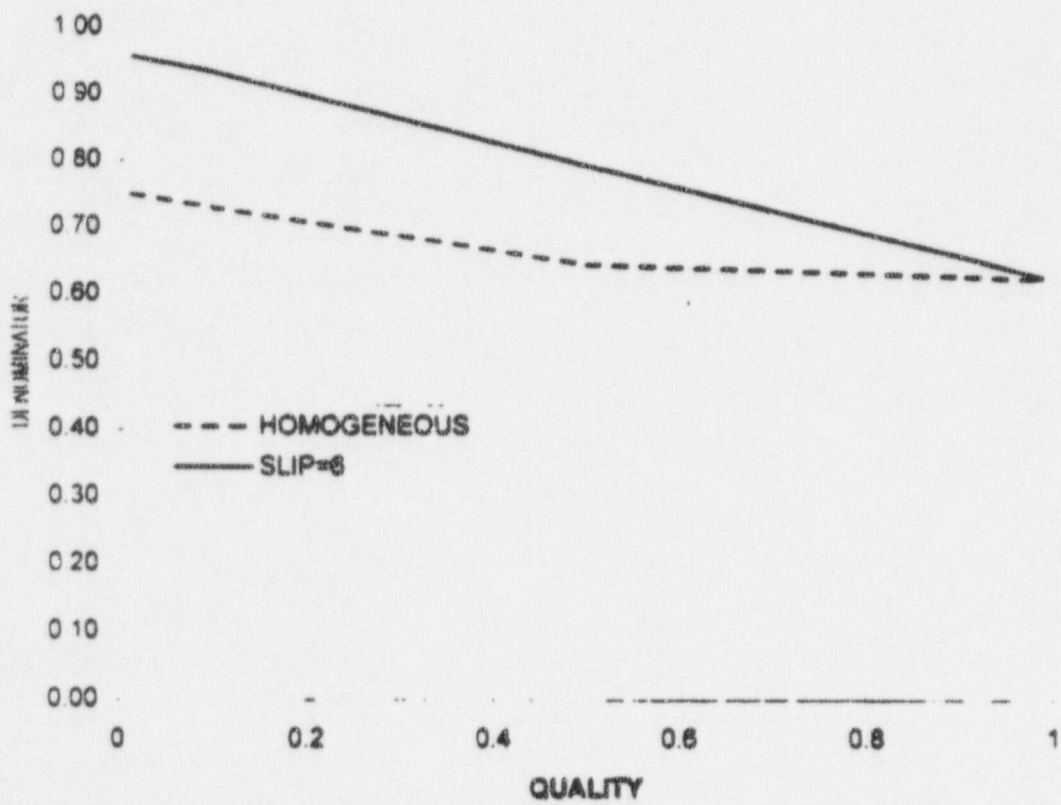


Figure 1.7-6 Effect of Slip Ratio on Momentum Flux Equation Denominator

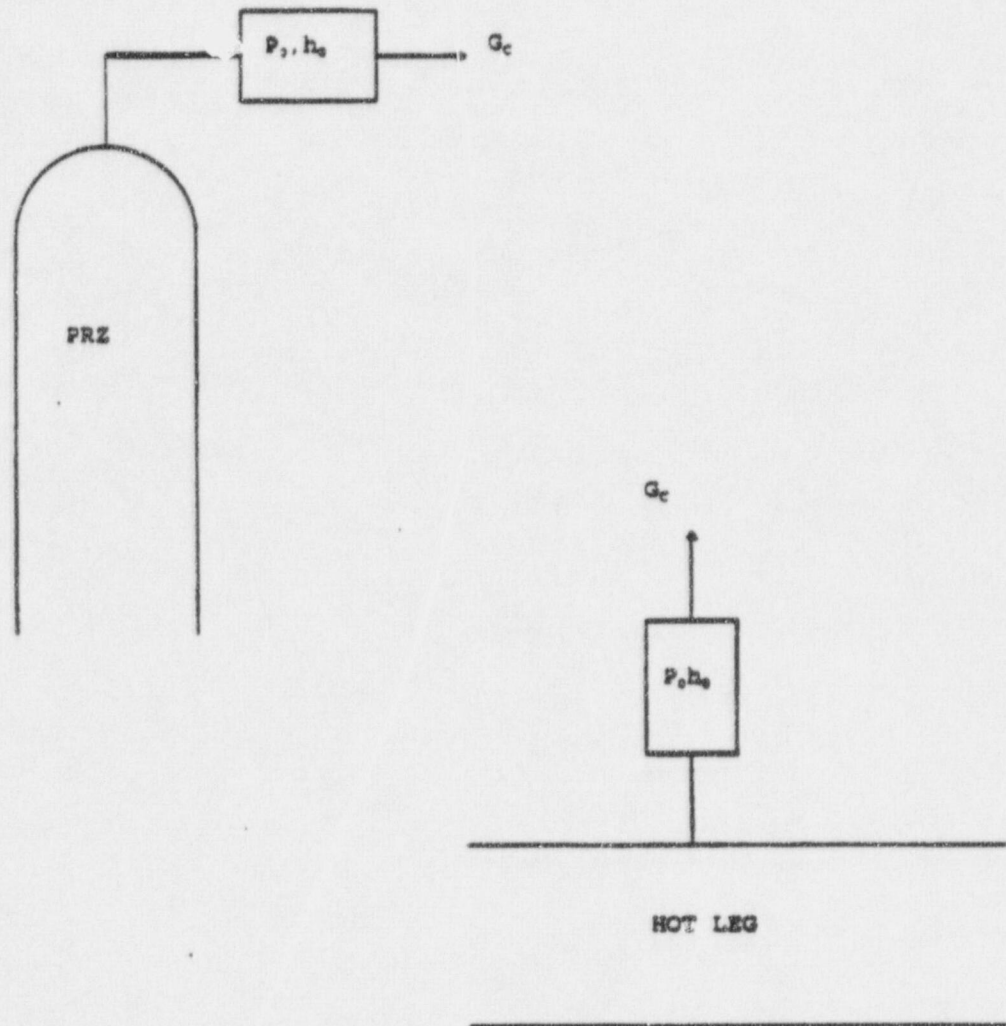


Figure 1.7-7 NOTRUMP Noding for ADS Valves

Net Expansion Factor Y for Compressible Flow Through Pipe to a Larger Flow Area

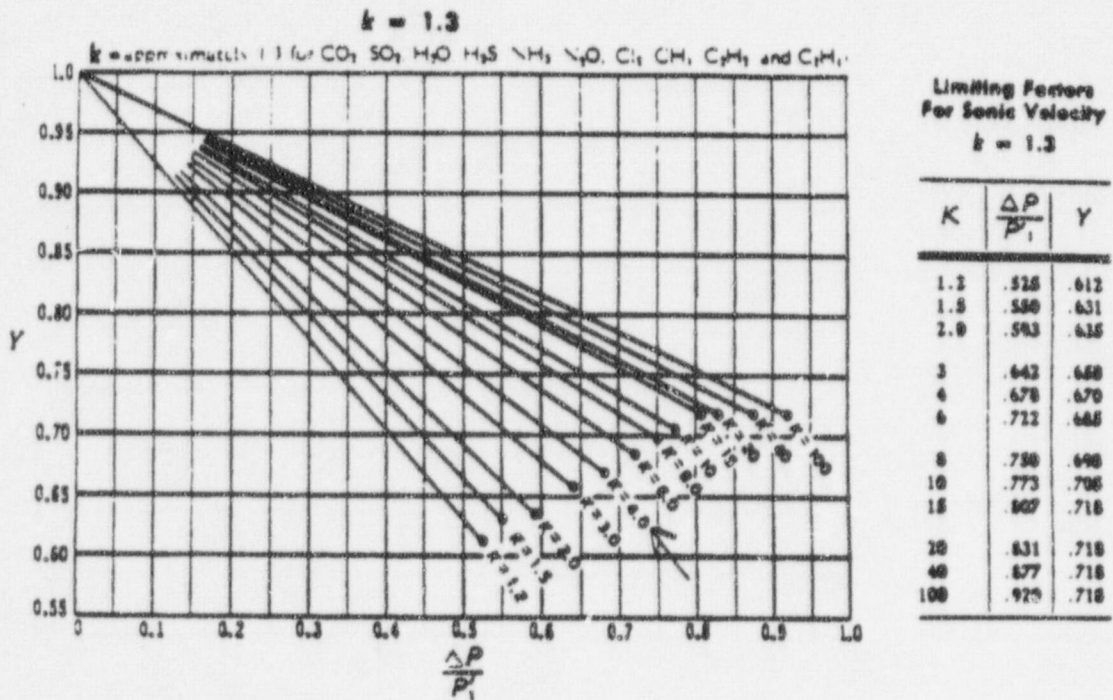


Figure 1.7-8 Effect of Compressibility on the Calculated Flowrate Through a Piping System

ADS4 FLOW VS PRESSURE USING COMPRESSIBILITY FACTOR

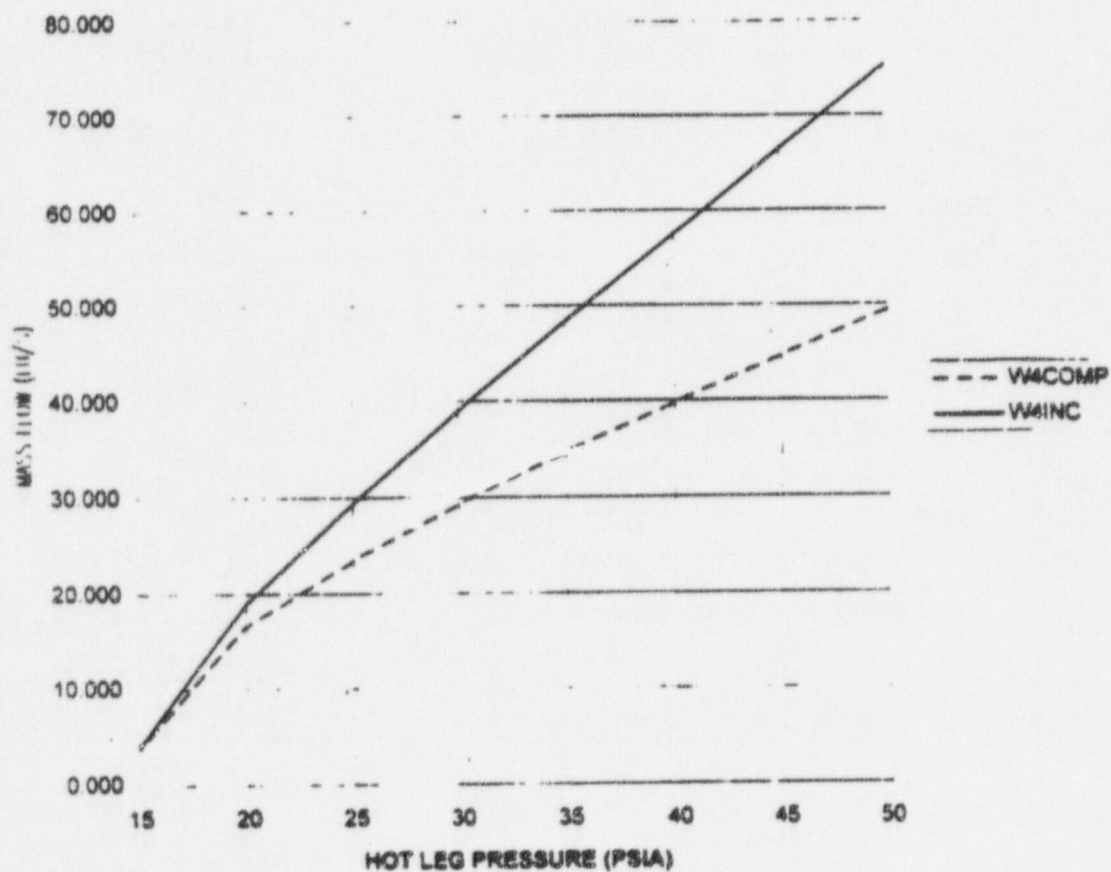


Figure 1.7-9 Effect of Compressibility on ADS4 Flow vs. Pressure

AP600 2INBREAK IN FNODE 49 12 node core
 Mass Flow Rate (lbm/s)
 △ WGFL 185 0 0 ADS 4A VAPOUR FLOW
 Mass Flow Rate (lbm/s)
 - - - - Blending Value

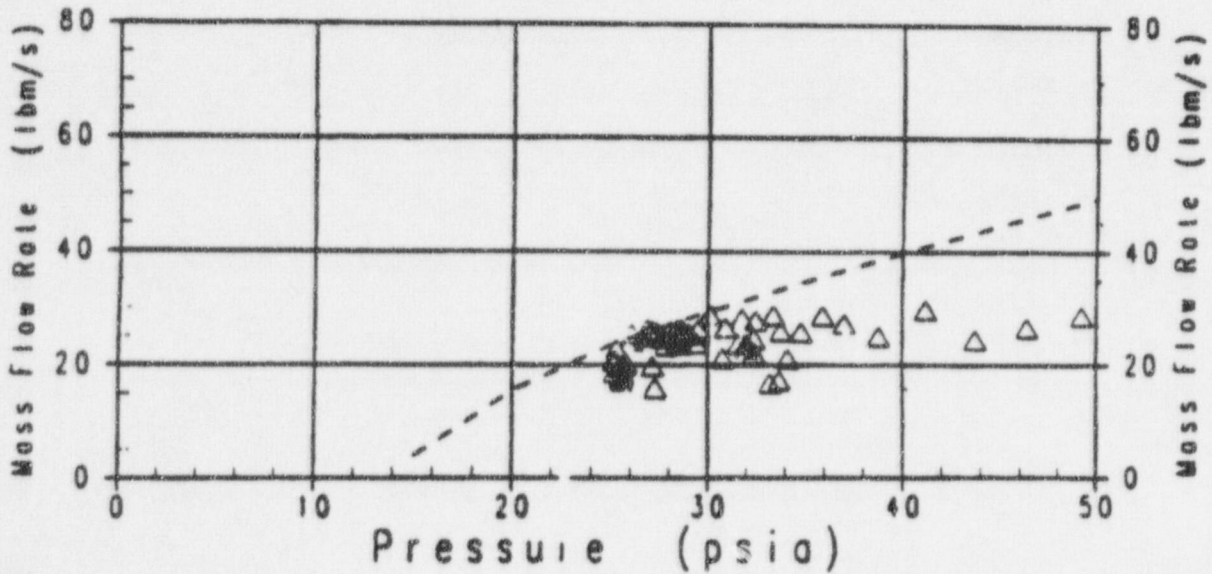


Figure 1.7-10 NOTRUMP Predicted Vapor Flow Compared with Reference 1-23 Calculation

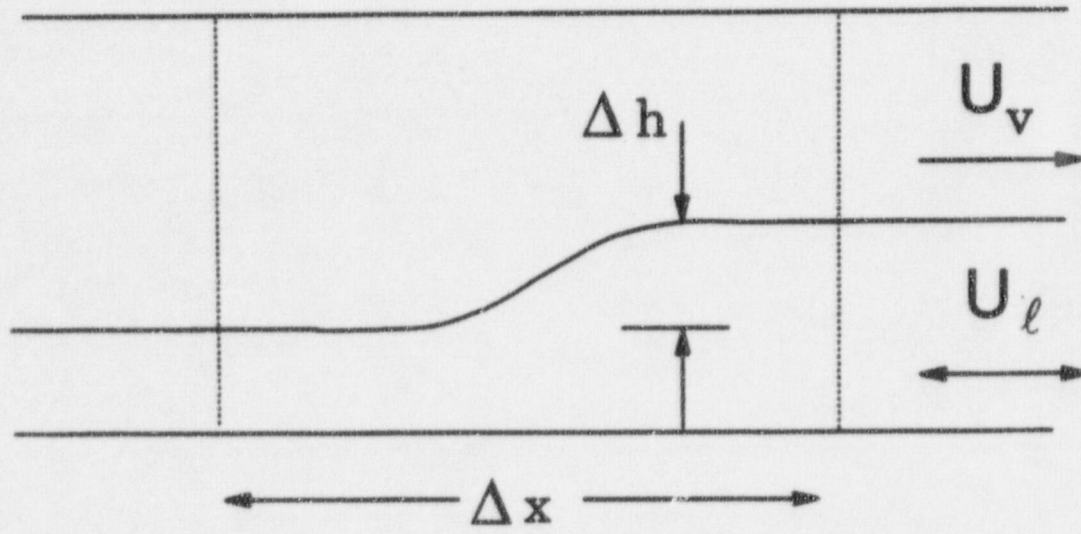
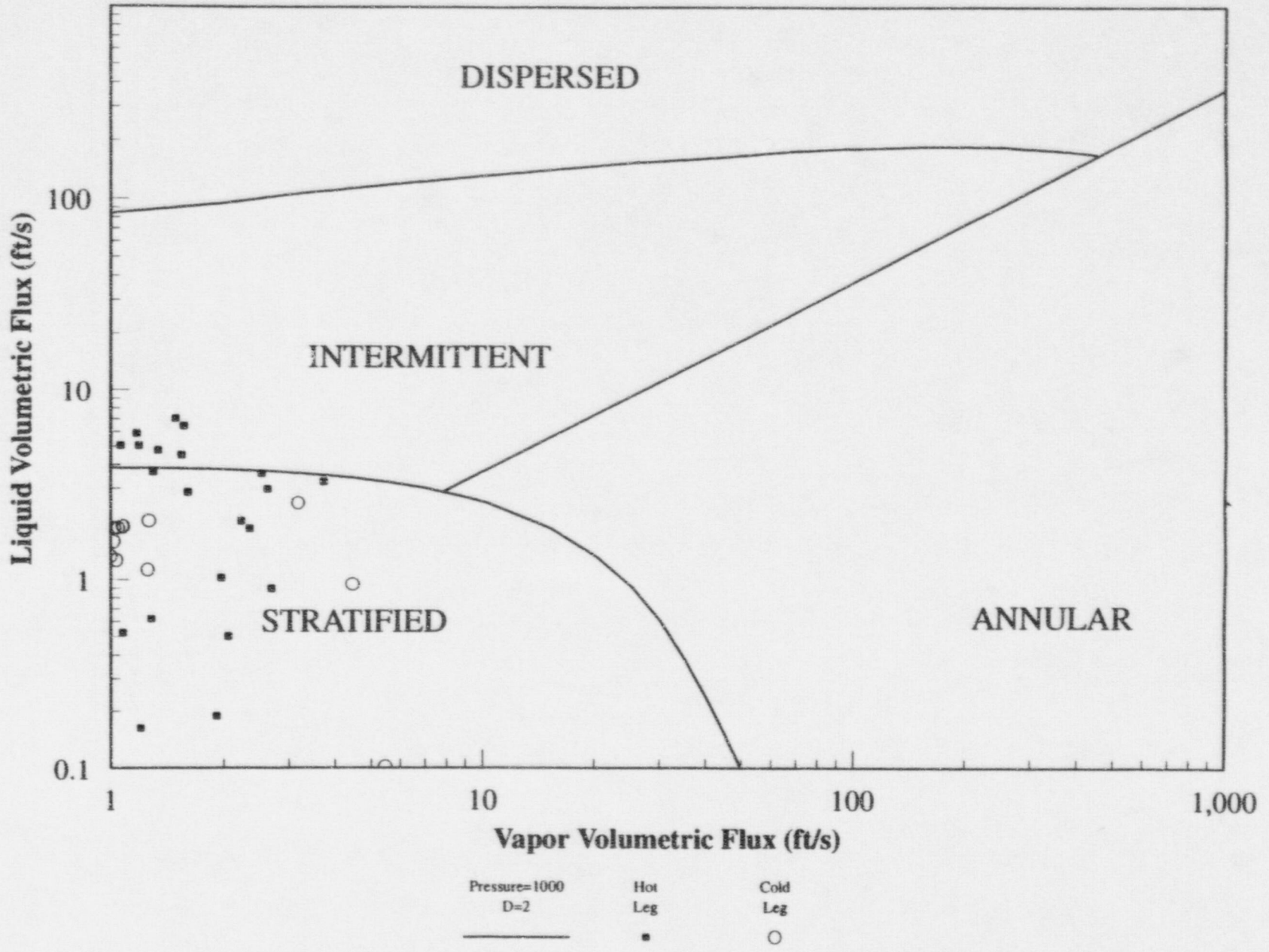


Figure 1.7-11 Horizontal Stratified Flow with Level Gradient

Figure 1.7-12 Flow Regimes in Hot Leg and Cold Leg (High Pressure, Prior to ADS Opening)



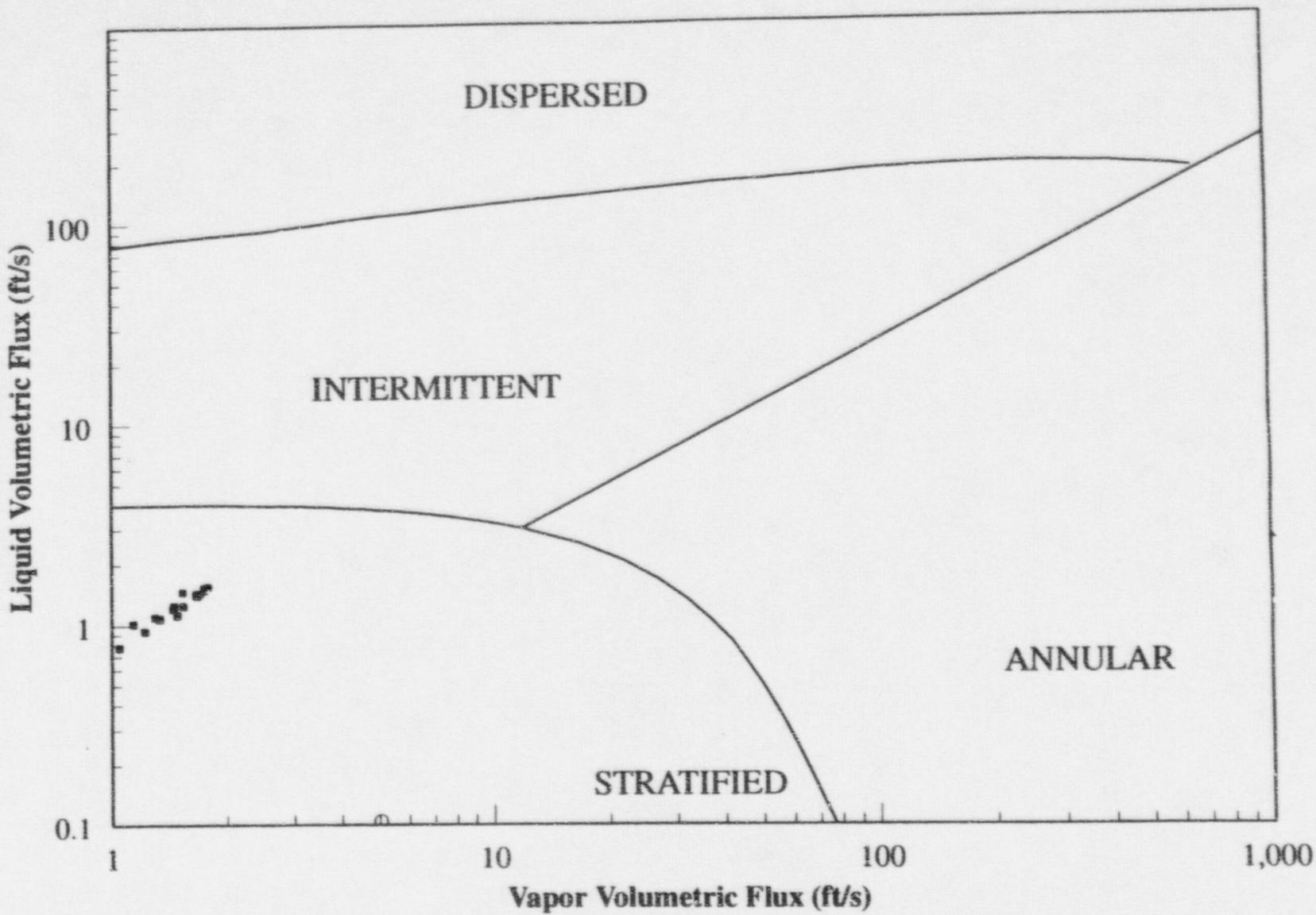


Figure 1.7-13 Flow Regimes in Hot Leg and Cold Leg (Intermediate Pressure, Just After ADS Opening)

Figure 1.7-15 Flow Regimes in Balance Line (High Pressure, Just Prior to ADS Opening)

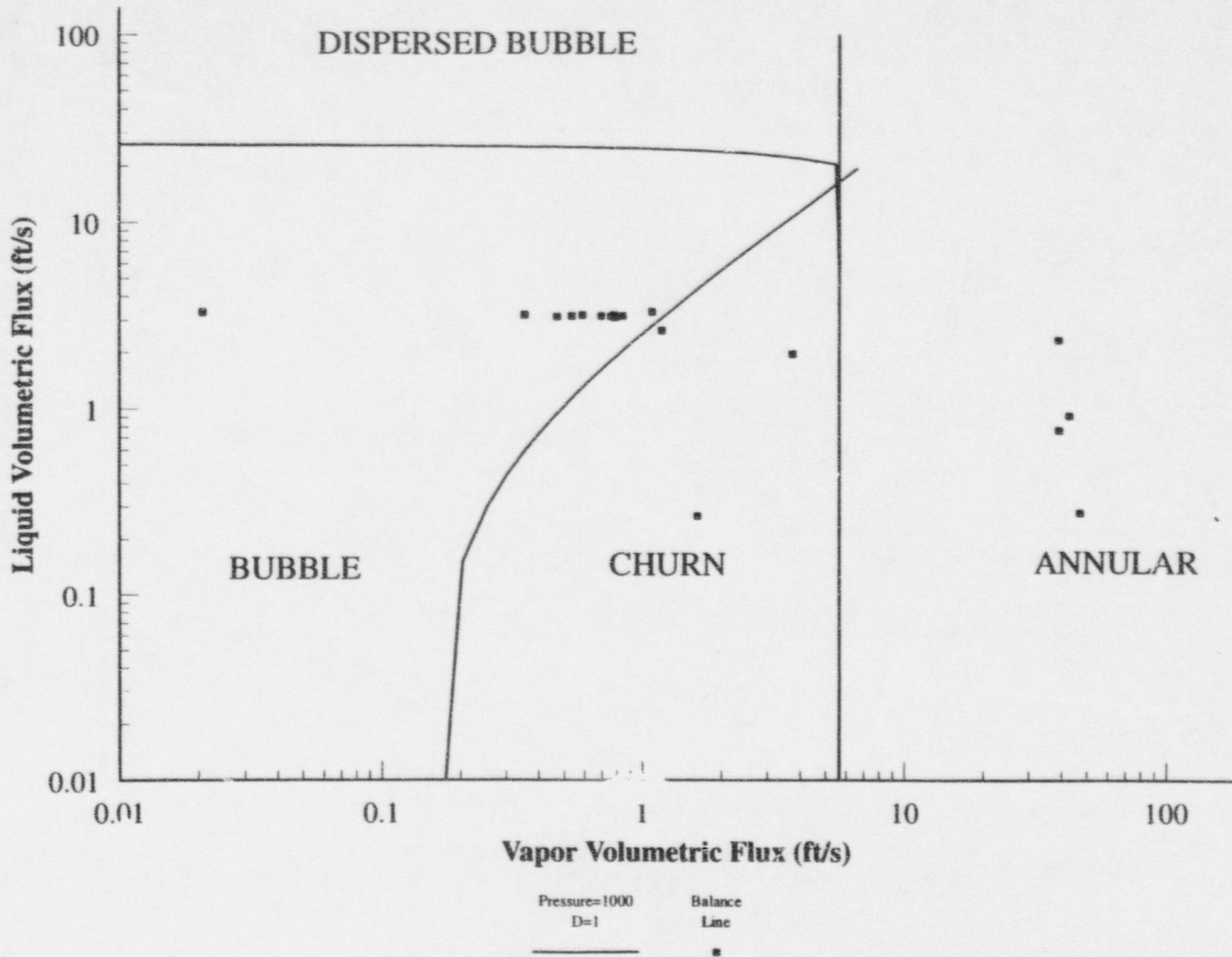
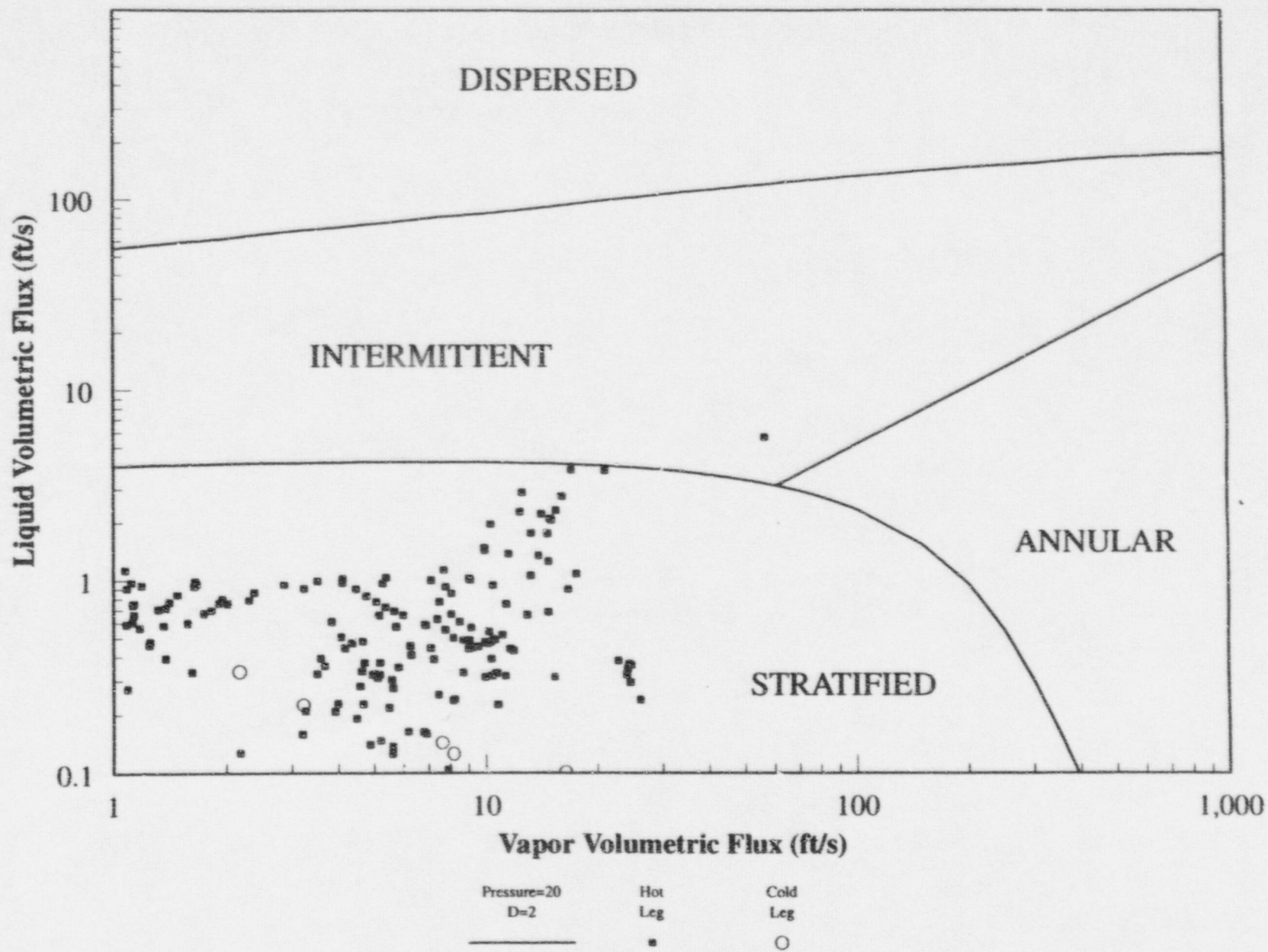
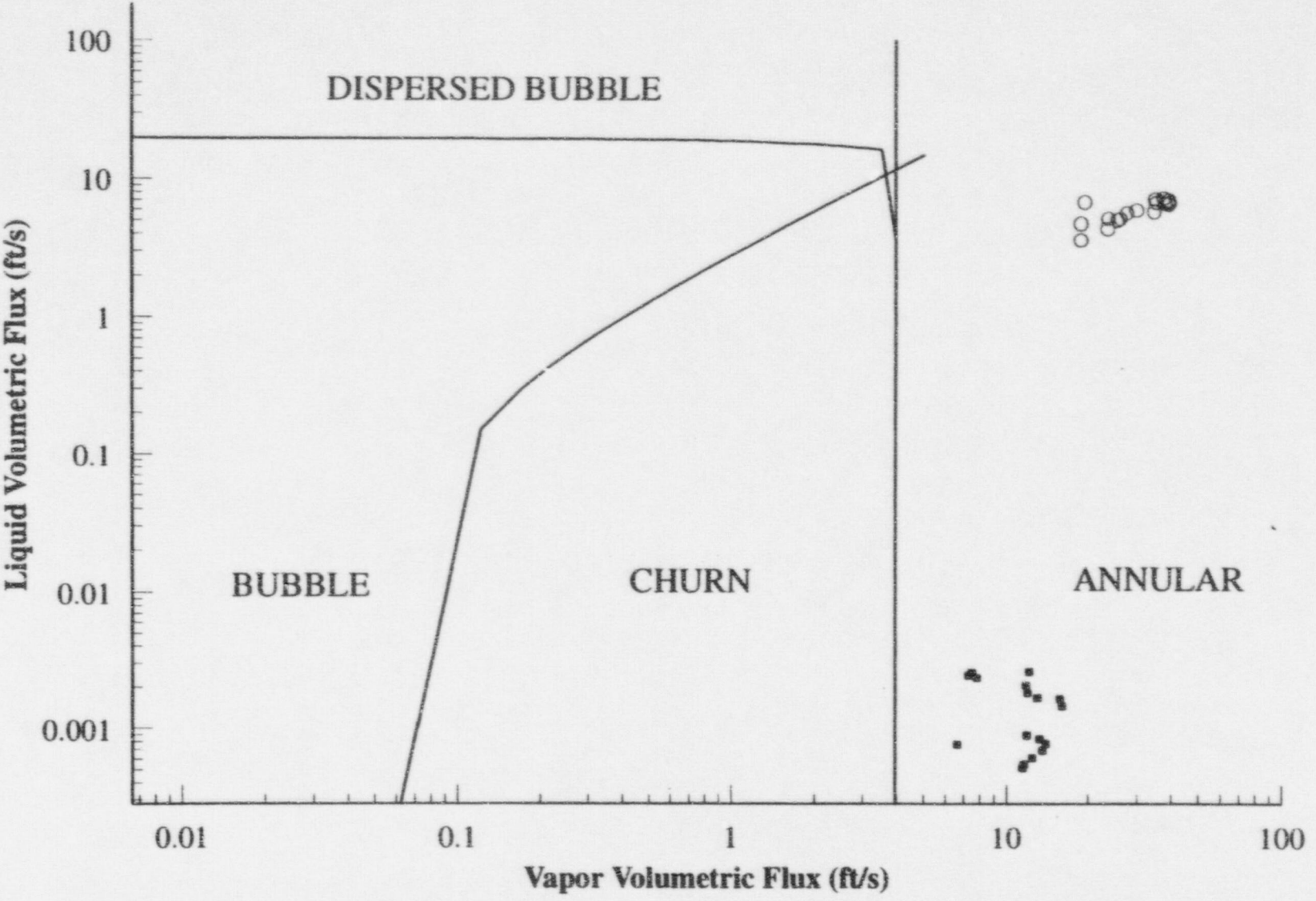


Figure 1.7-14 Flow Regimes in Hot Leg and Cold Leg (Low Pressure)





Pressure=500
D=1

Balance Line Surge Line

■ ○

Figure 1.7-16 Flow Regimes in Balance Line and Pressurizer Surge Line (Intermediate Pressure, Just After ADS Opening)

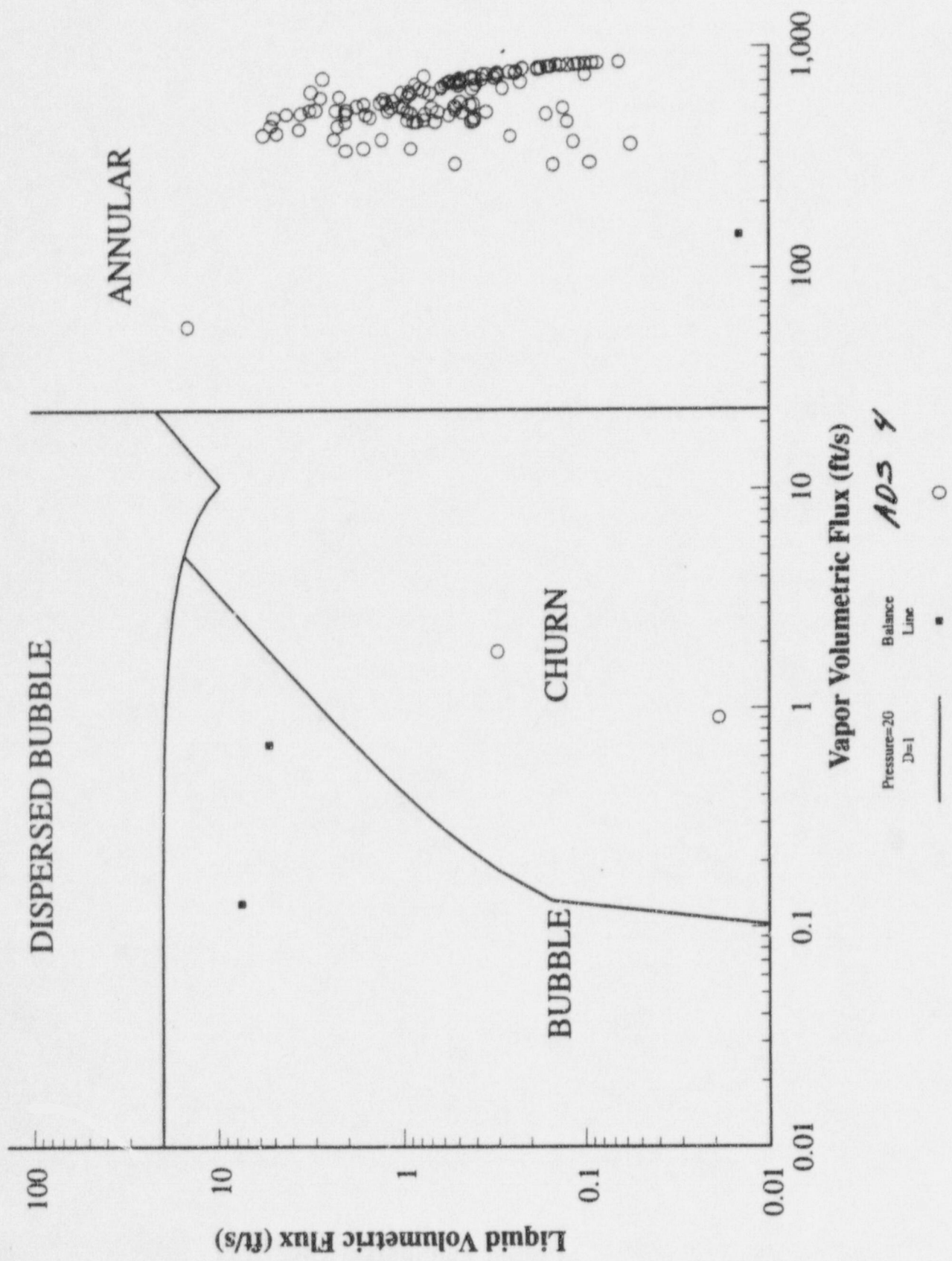
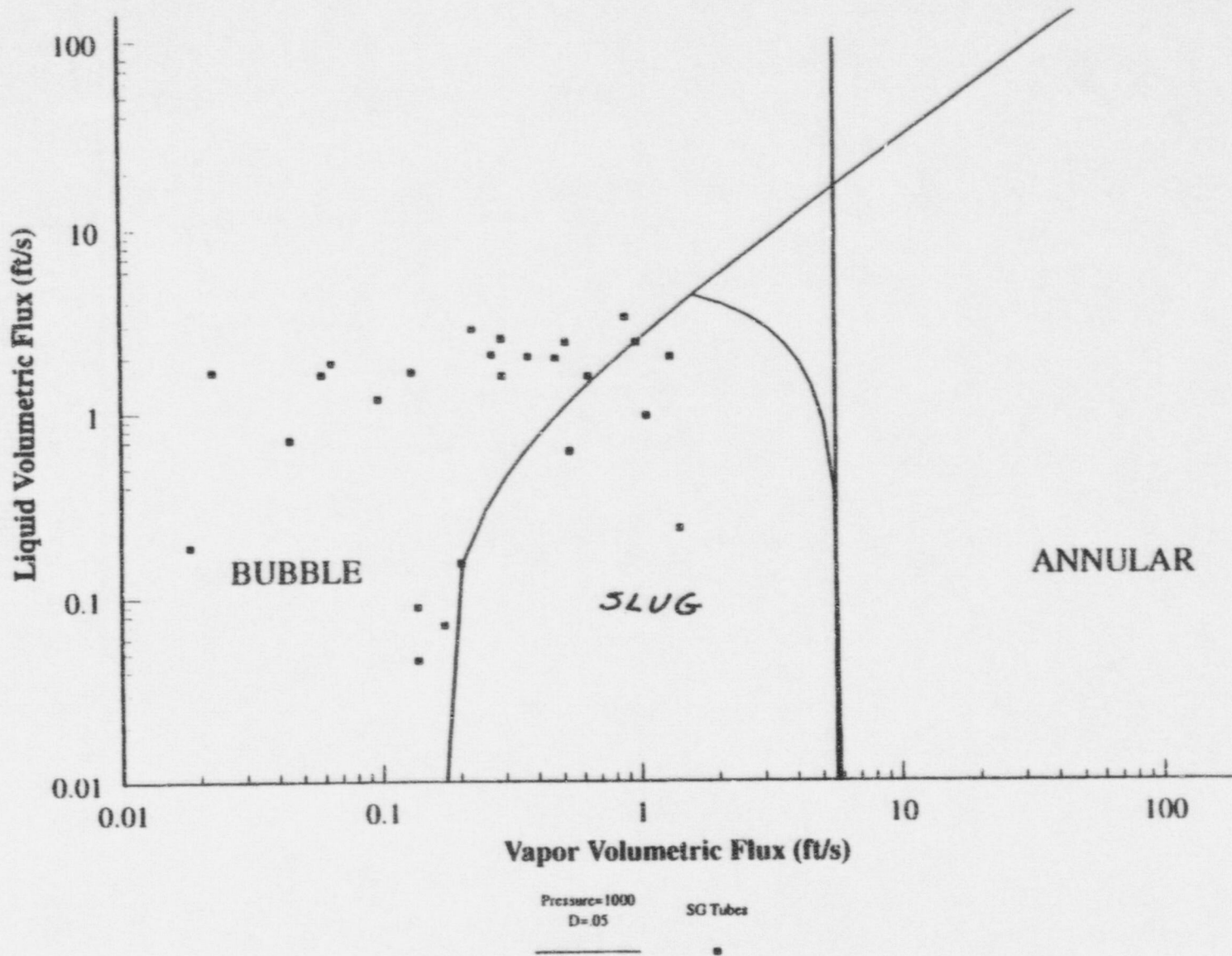


Figure 1.7-17 Flow Regimes in Balance Line and ADS-4 (Low Pressure)

Figure 1.7-18 Flow Regimes in Steam Generator Tubes (High Pressure, Just Prior to ADS Opening)



1.17 Key Features of the AP600 Analysis Methodology

The application of NOTRUMP as an Appendix K evaluation model to the AP600 must take into account the findings from the assessment described in this report. First, the following conservative features required by Appendix K are applied:

a) Appendix K requirements

ANS 71 + 20 percent core decay heat

Application of this model increases the core power by nearly 25 percent compared with the more recent 1979 ANS standard for decay heat, during the time period of most interest near the point of ADS-4 actuation. Since the mass inventory and system pressure is in large part determined by the steam generation rate, application of this model leads to significant conservatism.

Moody critical flow model at the break and break spectrum

Application of the Moody model results in overprediction of the break flow by about 20 percent relative to data. The integral effects tests confirm that larger breaks tend to reduce system mass to a greater extent than smaller breaks. This model therefore is also considered to include additional conservatism, when combined with the required analysis of a spectrum of breaks.

b) Additional Conservatisms to Account for Plant Geometry Uncertainties

The resistances in the DVI, IRWST, CMT, and accumulator lines are set at design upper bound values to reduce the flow rate from the passive components into the RCS. In addition, the minimum effective critical flow area is used in the ADS critical flow calculation, and maximum resistances are used in the ADS flow paths.

Minimum containment pressure (14.7 psia) is assumed.

c) **Additional Confirmatory Checks and Assumptions to Account for Model Deficiencies**

Table 1.17-1 summarizes the highly ranked component phenomena from the PIRT (Table 1.3-1) and the results of the assessment performed in this report. In several areas, model deficiencies in NOTRUMP resulted in minimal agreement with the data. The reasons for the minimal agreement are also given. For each area where agreement was minimal, the actions taken into account for the deficiency in the AP600 analysis are also given. The three specific actions to be taken are:

1. The flow velocity through the PRHR primary will be confirmed to be less than 1.5 ft./sec in all AP600 simulations. In addition, the PRHR is removed from the model after ADS 1-3 actuation to further reduce the depressurization rate.
2. If the flow through the PRHR is higher than 1.5 ft./sec. for any significant period of time, the calculation for the limiting case (minimum mass or highest PCT) is repeated with the PRHR heat transfer surface area reduced by 50 percent to account for the potential overprediction of heat transfer.
3. The IRWST flow will be delayed to account for potential nonconservatism in the prediction of system pressure after ADS-4 actuation. This will be accomplished by reducing the IRWST level by 6 feet. The basis for this value is described in the response to RAI 440.721(g).

In summary, the differences between predicted and actual integral test results can be attributed to one or more of the identified model deficiencies discussed in this report. For those areas where the agreement was found to be minimal, specific steps have been taken to address the deficiency in the AP600 analysis.

**TABLE 1.17-1
ASSESSMENT SUMMARY**

Component Phenomenon	Assessment Results	How Treated in AP600 Analysis	Comments
ADS 1-3:			
Critical flow	Reasonable; provided correct reservoir conditions are calculated	Minimum critical flow areas	ADS1-3 inlet quality too high because PRZR level swell is underpredicted; result is under prediction of ADS1-3 flow
Two-Phase Pressure drop	Reasonable	Upper bound loss coefficients	Lack of momentum flux terms in ADS 1-3 results in small error
Valve loss coefficients	N/A	Upper bound loss coefficients obtained from valve tests	
ADS4:			
Two-phase pressure drop	Minimal; due to lack of momentum flux terms, underpredicted pressure drop	Apply IRWST level penalty ¹ Upper bound loss coefficients	Flow out ADS4 is overpredicted, resulting in early PRZR drain and IRWST initiation
BREAK:			
Critical flow	Reasonable; provided reservoir quality is correctly predicted	Moody model used. Break size, location ranged ²	Low-level swell results in lower quality flow at break; total system mass is under predicted

¹ Level penalty is indirect correction for most significant deficiency, lack of momentum flux in ADS4. All SAR cases run with increased ADS4 resistance to confirm level penalty approach.

² Additional studies ranging CD for break.

**TABLE 1.17-1
ASSESSMENT SUMMARY (Cont.)**

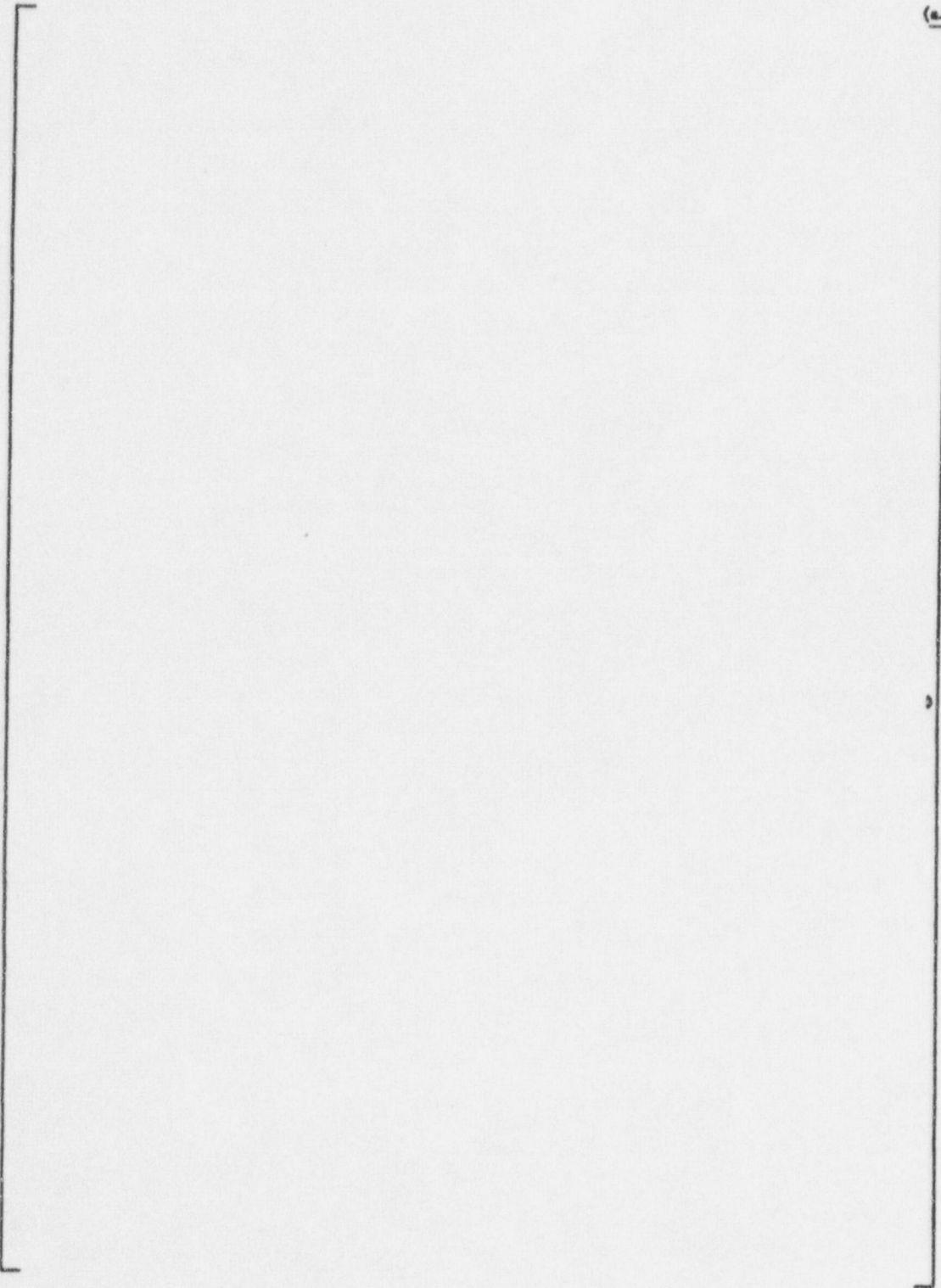
Component Phenomenon	Assessment Results	How Treated in AP600 Analysis	Comments
ACCUMULATORS:			
Injection flow	Reasonable	Upper bound loss coefficients Maximum water temperature	
COLD LEGS:			
Phase separation at tees	Minimal, but conservative	No change	Balance line refilling delays CMT drain
VESSEL/CORE:			
Decay heat	N/A	1971 +20% ANS used.	
Natural circulation flow	Reasonable	No change	
Mixture level	Conservative if core uncovers	No change	Mixture level underpredicted in boil-off experiments
CMT:			
Circulation	Excellent	No change	
Thermal Stratification	Minimal, but conservative	No change	Lack of model increases CMT exit temperature, reduces core subcooling
Draining	Reasonable	No change	Some evidence of delayed flashing (non-equilibrium) in 1/2 inch break; judged no important

**TABLE 1.17-1
ASSESSMENT SUMMARY (Cont.)**

Component Phenomenon	Assessment Results	How Treated in AP600 Analysis	Comments
DOWNCOMER:			
Level	Minimal for DEDVI	Apply IRWST level penalty Range CD for break to assure limiting case found	Downcomer model does not predict 2-D temperatures. Excess condensation during IRWST.
HOT LEGS:			
Stratifications, phase separation at tees	Minimal due to ad hoc model; impact is small	Apply IRWST level penalty	Liquid flow out ADS4 is controlled by constant system inventory, inlet flows, self correcting system
IRWST:			
Gravity draining	Reasonable	Use upper bound line resistance Maximum water temperature	High IRWST flow in OSU due to PRZ draining, downcomer condensation
PRESSURIZER AND SURGE LINE:			
CCFL	Minimal but conservative provided vapor flow is correct	No change; given correct or high vapor flow, CCFL is conservative	Rapid draining through surge line caused by low vapor flow due to low pressure drop through ADS4
Entrainment (above mixture level)	Reasonable	No change	Low ADS1-3 mass flow is due to low level swell, not entrainment above the mixture level
Level Swell	Minimal non-conservative during draining	Apply IRWST level penalty	Rapid draining due to poor ADS4 pressure drop prediction; confirmed by studies with increased ADS4 resistance

**TABLE 1.17-1
ASSESSMENT SUMMARY (Cont.)**

Component Phenomenon	Assessment Results	How Treated in AP600 Analysis	Comments
STEAM GENERATOR:			
Natural circulation	Reasonable	No change	
Heat transfer	Minimal	No change	Underprediction in PRHR, CMT increases SG heat transfer
Tube draining	Reasonable	No change	
PRHR:			
Heat transfer	Minimal, conservative if primary flow is low	Remove PRHR after ADS3, check PRHR flow	Heat transfer not overpredicted as long as primary side is limiting
Recirculation flow	Minimal, conservative if primary flow is low	Remove PRHR after ADS3, check PRHR flow	Under predicted flow reduces PRHR heat transfer
UPPER HEAD/ UPPER PLENUM:			
Mixture level	Reasonable	No change	



(s.b.c)

OSU Test Sb18 2 Inch Cold Leg Break

Collapsed Downcomer Levels (Relative to Bottom of Lower Plenum)

— Test Data
- - - NOTRUMP Simulation

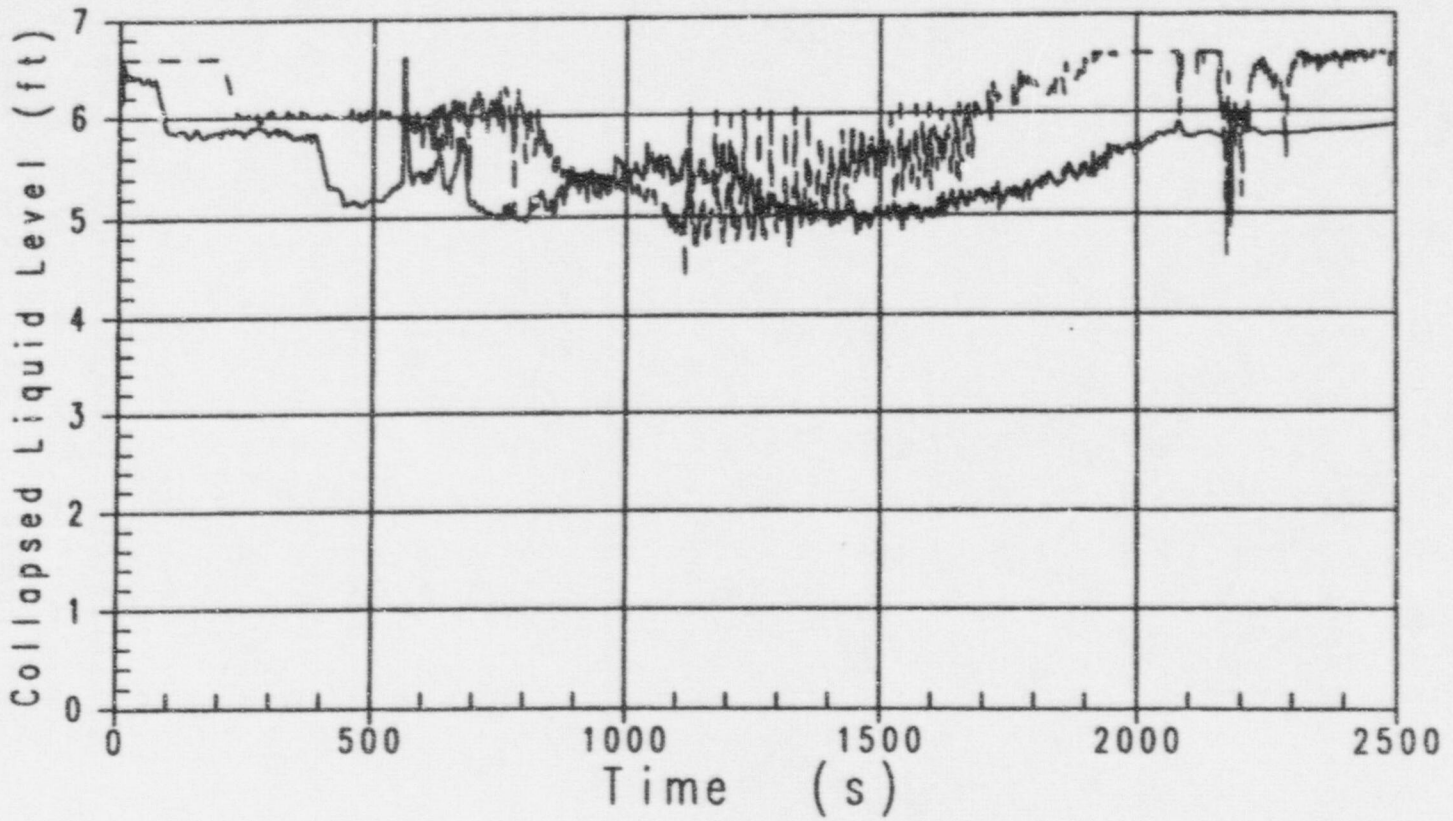


Figure 8.3.1-18

OSU Test Sb18 2 Inch Cold Leg Break
Integrated Break Flow

— Test Data
- - - NOTRUMP Simulation

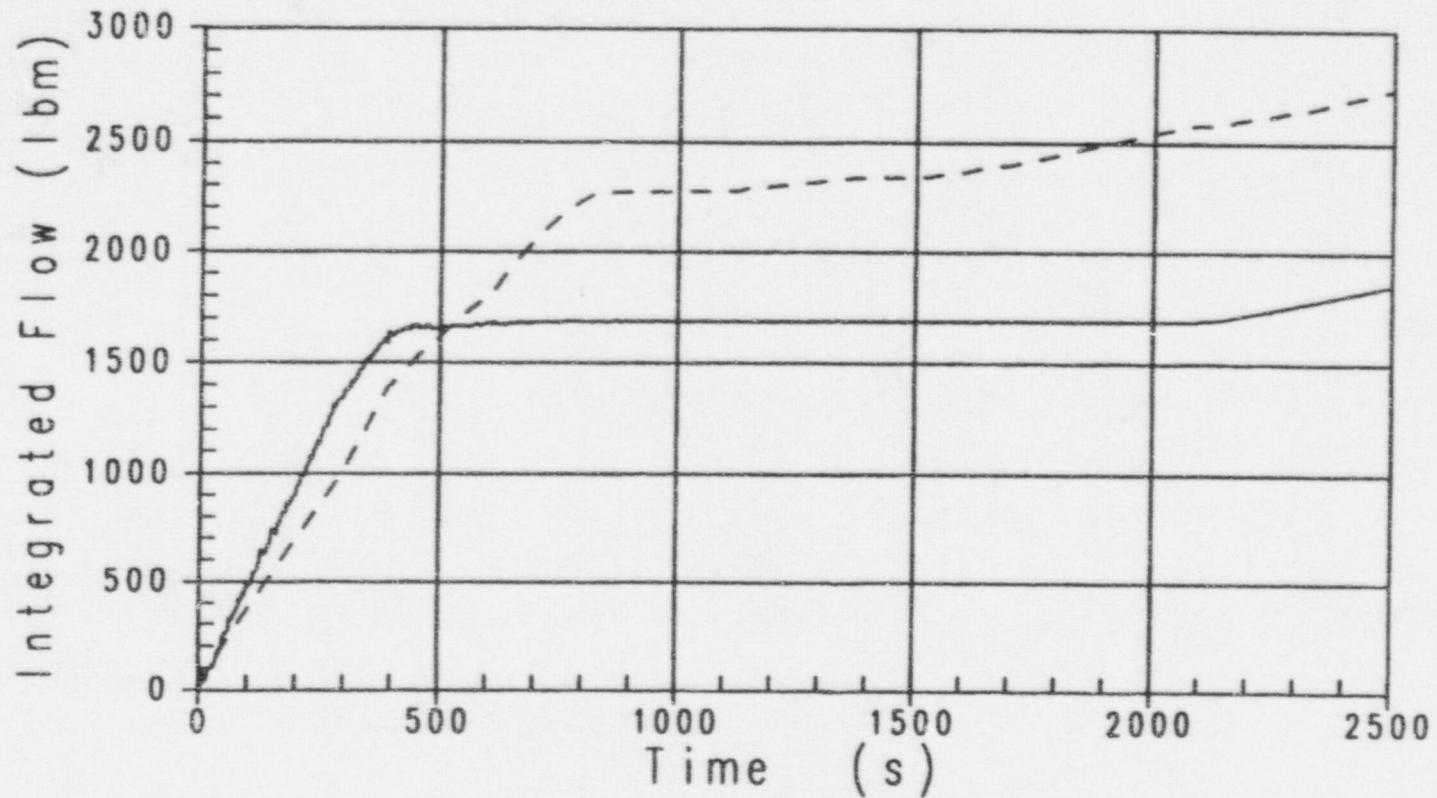
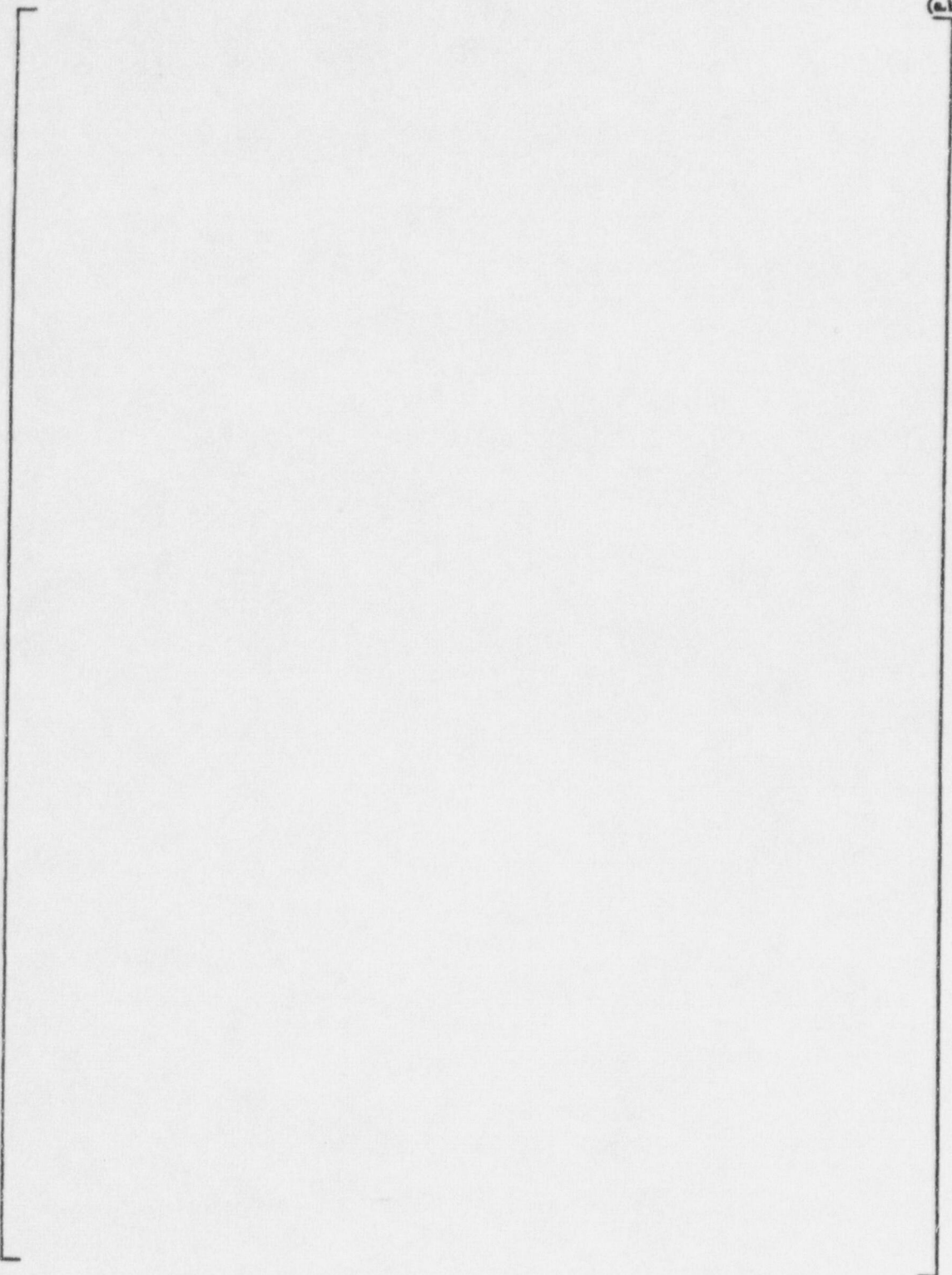
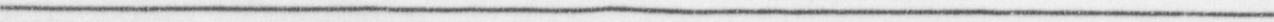


Figure 8.3.1-29



(a.b.c)